

1 **Tidal mixing maintains regional differences in water**
2 **properties and nutrient ratios in British Columbia**
3 **coastal waters**

4 **H. V. Dosser¹, S. Waterman¹, J. M. Jackson², C. G. Hannah³, B. P. V.**
5 **Hunt^{1,4,5}**

6 ¹Department of Earth, Ocean and Atmospheric Sciences, University of British Columbia, Vancouver, BC,
7 V6T 1Z4

8 ²Hakai Institute, 1010 Langley St, Victoria, BC, V8W 1V8

9 ³Fisheries and Oceans Canada, Institute of Ocean Sciences, Sidney, BC, V8L 4B2

10 ⁴Institute for the Oceans and Fisheries, University of British Columbia, Vancouver, BC, V6T 1Z4

11 ⁵Hakai Institute, Heriot Bay, Quadra Island, BC, V0P 1H0

12 **Key Points:**

- 13 • An abrupt and persistent lateral gradient in water properties is quantified, co-located
14 with strong tidal mixing bisecting the study area.
- 15 • Differences in the seasonality, open-ocean connectivity, and response to stressors
16 are found in the regions separated by the tidal mixing.
- 17 • The mixing is likely limiting the two-layer estuarine exchange flow between regions,
18 and so modifying the transport pathways for nutrients.

Corresponding author: Hayley V. Dosser, hdosser@eoas.ubc.ca

Abstract

Tidal mixing is recognized as a key mechanism in setting water properties in coastal regions globally. Our study focuses on Canada's British Columbia coastal waters, from Queen Charlotte Strait to the Strait of Georgia. This area is bisected by a region of exceptionally strong mixing driven by some of the strongest tidal currents in the world. We examine the influence of this tidal mixing on regional differences in water properties and nutrient ratios. Our results quantify a spatially-abrupt and temporally-persistent lateral gradient in temperature, salinity, and density co-located with the region of strongest mixing. The distributions of density on either side of this front remain largely distinct throughout the spring-neap tidal cycle, year-round, and for over 70 individual years for which data are available. Additionally, nutrient molar ratios north of the front are statistically distinct from those to the south. Seasonal changes driven by the arrival of upwelled water differ in both timing and magnitude on either side of the front. Taken together, these results indicate limited exchange of water through the region of strongest tidal mixing, and suggest that Queen Charlotte Strait and the Strait of Georgia are largely isolated from each other. As such, this area provides a valuable case study for the degree to which the reduction of estuarine exchange by tidal mixing can maintain abrupt and substantial regional differences in physical and biogeochemical water properties. Further, it demonstrates the potential of tidal mixing to modify nutrient transport pathways, with implications for marine ecosystems.

Plain Language Summary

Mixing caused by the tides affects properties in coastal waters globally. Our study focuses on coastal waters in British Columbia Canada, from Queen Charlotte Strait to the Strait of Georgia. This area is bisected by a region of strong mixing caused by some of the strongest tidal currents in the world. We examine how this tidal mixing affects water properties. Our results show that temperature, salinity, density, and the relative proportions of key nutrients change significantly across the region of strongest mixing. These differences between the two halves of the study area persist throughout the tidal cycle and year-round, for over 70 individual years. We also find differences in the seasonal cycles in properties and their similarity to open ocean waters. These results indicate that the exchange of water through the region of strongest tidal mixing is significantly limited, which suggests that Queen Charlotte Strait and the Strait of Georgia

51 are largely isolated from each other. As such, this area provides a valuable case study
52 for the ability of tidal mixing to maintain abrupt and substantial regional differences in
53 water properties. Further, it suggests that tidal mixing can affect nutrient transport to
54 different regions, an important consideration for marine ecosystems.

55 **1 Introduction**

56 Tidal mixing has been widely shown to play an important role in the modification
57 of coastal water properties and the maintenance of persistent tidal fronts, leading to dis-
58 tinct physical and biogeochemical properties in adjacent regions (Thomson, 1981; LeBlond,
59 1983; van Heijst, 1986; Loder et al., 1994). In many cases, tidal mixing can limit the es-
60 tuarine exchange flow typical of coastal waters (e.g. Waldichuk, 1957; Griffin & LeBlond,
61 1990; Masson, 2002; MacCready & Geyer, 2010; Johannessen et al., 2014) reducing the
62 transport of properties between regions. The resulting regional differences in water prop-
63 erties have direct effects on marine ecosystem function, including primary and secondary
64 productivity, the location of biological hotspots, and the connectivity of ecosystems (Harrison
65 et al., 1983; Gay & Vaughan, 2001; Arimitsu et al., 2016).

66 The influence of tidal mixing is expected to be particularly significant on the south-
67 western coast of British Columbia (BC) Canada, an area where rapid tidal currents and
68 complex topography force some of the strongest tidally-driven turbulence in the world
69 (e.g. Foreman et al., 2012). Our specific study area along the BC coast is located to the
70 east and north of Vancouver Island; from eastern Queen Charlotte Strait (QCSt) through
71 Johnstone Strait (JS) and the Discovery Islands (DI) into the northern Strait of Geor-
72 gia (SoG) (Figure 1). Strong tidal currents in the study area are well-documented, as
73 is the resulting intense turbulent mixing over rough bathymetry and sills (Thomson, 1981;
74 Griffin & LeBlond, 1990; Foreman et al., 2004). In particular, the shallow, narrow chan-
75 nels in eastern JS and the DI that bisect the study area are known to have the strongest
76 tidal currents in Canada, driving the most intense turbulence in Canadian waters (Whitney
77 et al., 2005).

78 Southwestern British Columbia’s complex topography was carved out by glaciers,
79 and is characterized by fjords, islands, inlets and straits. The tidal currents are mixed,
80 dominantly semidiurnal, and propagate both north and south around Vancouver Island
81 before meeting in the area between QCSt and the SoG (Thomson, 1981). A two-layer

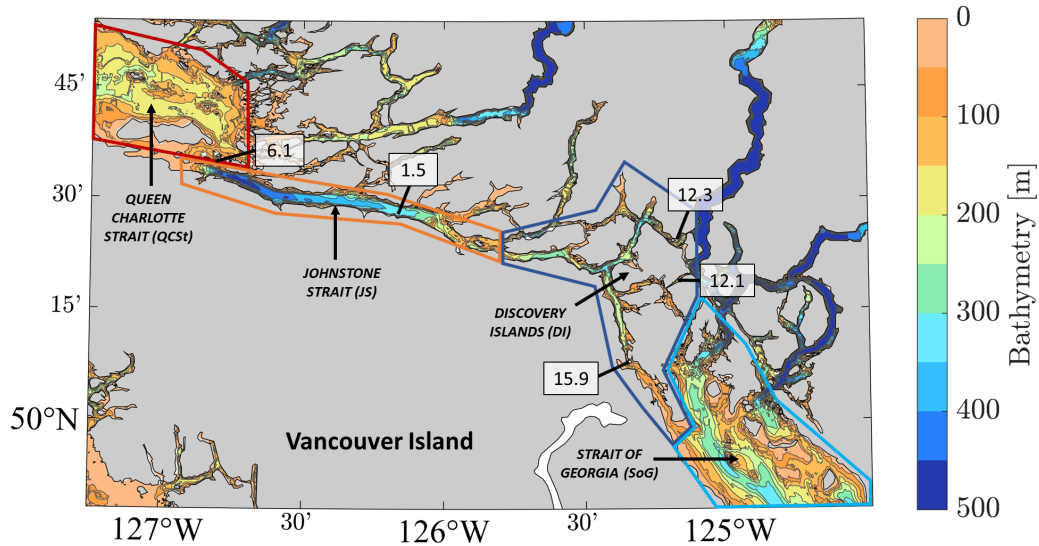


Figure 1. Bathymetric map of the study area showing the boundaries of the four regions: eastern Queen Charlotte Strait (QCSt, red), western Johnstone Strait (JS, orange), the Discovery Islands region (DI, dark blue), and the northern Strait of Georgia (SoG, light blue). The maximum tidal currents (in knots) in select passages are given (*Canadian Tide and Current Tables / Tables des marées et courants du Canada*, 2019).

82 estuarine circulation is driven by surface outflow from numerous terrestrial freshwater
 83 sources, with stratification in the area controlled primarily by salinity. Reviews of the
 84 physical oceanography of the area are provided by Thomson (1981); LeBlond (1983); Whit-
 85 ney et al. (2005) and Riche et al. (2014). Similar complex coastal marine environments
 86 are encountered in Alaska, the south-west coast of Chile, New Zealand, and Scandinavia
 87 (e.g. Stanton & Pickard, 1980; Svendsen, 1995; Iriarte et al., 2014; Arimitsu et al., 2016).

88 Biological productivity in British Columbia's coastal waters is driven in part by
 89 the coastal upwelling of nutrient-rich deep ocean waters (Ware & McFarlane, 1989; Whit-
 90 ney et al., 2005). Specifically, nutrients in these coastal waters are replenished season-
 91 ally when large-scale wind patterns shift from downwelling- to upwelling-favorable, driv-
 92 ing a deep inflow of water from the Northeast Pacific Ocean. Nutrient molar ratios in
 93 these coastal waters can differ significantly from open ocean values due to modification
 94 by e.g., riverine inputs and denitrification in anoxic sediments (Smethie, 1987; Whitney
 95 et al., 2005). The influence of such modification is expected to vary regionally, partially
 96 as a result of tidal mixing limiting two-layer estuarine exchange flow and driving verti-

97 cal transport of nutrients towards the euphotic zone. Regional variations in the ratios
98 of nitrate, phosphate, and silicate can have significant implications for phytoplankton
99 species composition and productivity (Geider & La Roche, 2002; Arrigo, 2005; Strom
100 et al., 2006; Klausmeier et al., 2008).

101 An important effect of extremely vigorous tidal mixing on the circulation is to re-
102 move momentum from the two-layer estuarine exchange flow and enhance vertical mo-
103 mentum transfer (Griffin & LeBlond, 1990; Hibiya & LeBlond, 1993; Park & Kuo, 1996;
104 MacCready, 1999), causing a recirculation of inflowing water. In nearby Haro Strait, tidal
105 mixing is known to periodically drive such a recirculation, limiting estuarine exchange
106 and restricting deep inflow to occasional pulses of dense water passing over the sill be-
107 tween the Strait of Georgia and the Strait of Juan de Fuca (Griffin & LeBlond, 1990; LeBlond
108 et al., 1991; Hibiya & LeBlond, 1993; Masson, 2002; Masson & Cummins, 2004; Johan-
109 nessen et al., 2014). The impact of tidal mixing on circulation in our study area is ex-
110 pected to be even more pronounced, making this area an ideal case study for the poten-
111 tial of tidal mixing to drive sustained regional differences in physical and biogeochem-
112 ical water properties. Past studies by Thomson (1976) and Thomson (1981) showed ev-
113 idence of such a transition in properties in the study area, identifying a well-defined full-
114 depth density front co-located with the sill separating the shallower eastern end of JS
115 from the DI. The reduction of estuarine exchange, the recirculation of inflowing water,
116 and other impacts of tidal mixing are additionally expected to result in region-specific
117 ecosystem dynamics and responses to environmental stressors that presently affect the
118 study area, including ocean acidification (e.g. Feely et al., 2016; Evans et al., 2019), hy-
119 poxia (e.g. Crawford & Peña, 2013), and marine heatwaves (e.g. Di Lorenzo & Mantua,
120 2016; Jackson et al., 2018).

121 In this study, our goal is to robustly quantify regional differences in water prop-
122 erties and consider the implications for eastern Queen Charlotte Strait through to the
123 northern Strait of Georgia, transecting the region of intense tidal mixing in Johnstone
124 Strait and the Discovery Islands. To do so, we combine historic observations spanning
125 multiple decades with high-temporal resolution observations from recent years, thereby
126 creating a new regional data product for physical water properties and nutrient concen-
127 trations (Section 2). We use this data product to quantify spatial and temporal variabil-
128 ity in water properties to a previously inaccessible degree (Section 3), creating a com-
129 prehensive picture of the regional structure of physical water properties and nutrient ra-

130 tios. Finally, we discuss how these findings provide insight into the role of tidal mixing
131 in setting coastal ocean properties and maintaining regional separation, and further how
132 this mixing-induced regionalization can impact ecosystems (Section 4).

133 **2 Data and Methods**

134 From this point onwards, the abbreviations QCSt, JS, DI, and SoG will be used
135 to refer to the four regions shown in Figure 1. These useful subdivisions of our study area
136 are defined based on data availability, bathymetric features such as sills that provide nat-
137 ural boundaries, and stratification used as a proxy for the influence of mixing in each
138 region (see Supporting Information S.1 for a full discussion). In these regions, the far
139 eastern end of Johnstone Strait is included in the DI region, so that ‘JS’ refers strictly
140 to the western part of Johnstone Strait outlined in Figure 1. As such, the density front
141 in Johnstone Strait described in Thomson1976 and Thomson1981 and discussed herein
142 is co-located with the sill separating the JS and DI regions. We refer to this transition
143 zone between JS and the DI as the ‘tidal mixing frontal zone’.

144 **2.1 Data sources**

145 We quantify the spatial and temporal variability of physical and biogeochemical
146 water properties in the study area through the creation and analysis of a new data prod-
147 uct combining archived temperature (T), salinity (S), and nutrient concentration data
148 spanning multiple decades (Figure S2) collected by Fisheries and Oceans Canada (DFO)
149 and the University of British Columbia (UBC) with more recent data collected at high
150 temporal resolution by the Hakai Institute (Hakai). Details on these data sources are given
151 below and in Supporting Information S.2. Our analysis represents the first time that data
152 from these sources have been combined for this geographic area. The resulting data prod-
153 uct provides a combination of unparalleled spatial and temporal coverage over the re-
154 gions of interest, with sufficient temporal resolution in each region to investigate seasonal
155 variability in water properties (Figures S1, S2).

156 DFO has collected hydrographic temperature and salinity data in QCSt, JS, the
157 DI, and the SoG since the 1930s (*Institute of Ocean Sciences Data Archive*, 2020). Ad-
158 ditionally, UBC has collected hydrographic data in the study area since the 1970s. These
159 historic data were collected at locations spread across the study area during all months

160 of the year. In total, 3,269 DFO profiles and 1,138 UBC profiles are included in the new
161 data product and our analysis. Of these, 608 are from QCSt, 1,522 are from JS, 872 are
162 from the DI, and 1,405 are from the SoG. From the 1930s to the mid-1970s, tempera-
163 ture was measured using a reversing thermometer, while salinity was measured from wa-
164 ter samples. Beginning in the mid-1970s, use of a Conductivity-Temperature-Depth (CTD)
165 instrument equipped with electronic sensors to measure temperature, conductivity, and
166 pressure became common. The accuracy of the archived measurements is at minimum
167 0.1°C for temperature and 0.1 for CTD salinity. Salinity data collected pre-1980 using
168 bottle samples is comparable to recent CTD-based salinity data with an accuracy of 0.4
169 (Chandler et al., 2017).

170 More recently, from 2014 to present, the Hakai Institute has collected CTD data
171 in QCSt near the sill with JS, in the deep western end of JS, in the DI, and in the north-
172 ern SoG near Quadra Island where a Hakai field station is located. A total of 3,131 Hakai
173 CTD profiles are included in the data product and our analysis: this includes 103 pro-
174 files in QCSt, 244 profiles in JS, 353 profiles in the DI, and 2,431 profiles in the SoG. The
175 accuracy of these measurements is 0.005°C or better for temperature and 0.001 or bet-
176 ter for salinity.

177 Nutrient concentration data (nitrate+nitrite, phosphate, and silicate) collected by
178 DFO since 1977 are also included in our analysis (*Institute of Ocean Sciences Data Archive*,
179 2020). We use a total of 334 DFO nutrient profiles, with 48 profiles from QCSt, 46 pro-
180 files from JS, 61 profiles from the DI, and 179 profiles from the SoG. Here a ‘profile’ refers
181 to a set of samples collected at a single location for all three nutrients. Sample precision
182 is estimated to be $0.2\ \mu\text{mol L}^{-1}$ or better for nitrate+nitrite, $0.03\ \mu\text{mol L}^{-1}$ or better
183 for phosphate and $0.4\ \mu\text{mol L}^{-1}$ or better for silicate. Nutrient samples are not filtered
184 and were processed fresh until recent years, now most samples are processed frozen.

185 The DFO nutrient data are combined with Hakai Institute nitrate+nitrite, phos-
186 phate, and silicate concentration data collected at repeat sampling stations. These data
187 are available from 2014 onwards. A total of 909 Hakai nutrient profiles are used in the
188 analysis, with 102 profiles in QCSt, 189 profiles in JS, 79 profiles in the DI, and 539 pro-
189 files in the SoG. Sample precision is estimated to be $0.2\ \mu\text{mol L}^{-1}$ or better for nitrate+nitrite
190 (hereafter ‘nitrate’), $0.02\ \mu\text{mol L}^{-1}$ or better for phosphate and $0.2\ \mu\text{mol L}^{-1}$ or bet-
191 ter for silicate. Nutrient collection and processing protocols are identical to those cur-

192 rently used by DFO, with the exception that nutrients are filtered and are often collected
193 by small boat and so kept upright on ice in a cooler until they can be frozen to -20°C .

194 **2.2 Data interchangeability and sampling bias**

195 Our analysis of the new combined data product has the goals of quantifying per-
196 sistent regional differences in physical water properties and nutrient ratios, as well as re-
197 solving seasonal and depth variability in these regions. As such, interchangeability of data
198 from different sources is necessary, as is a careful consideration of biases in sampling.

199 The DFO, UBC, and Hakai data collection programs are independently run, and
200 the DFO data includes measurements collected by different internal programs (further
201 details provided in Chandler et al. (2017) and Supporting Information S.2). Previous stud-
202 ies that considered both DFO and Hakai hydrographic data sets suggest that the data
203 are comparable and can be used interchangeably (e.g. Jackson et al., 2018). Preliminary
204 comparisons (not shown) between nutrient samples collected by Hakai and DFO within
205 several days of each other at nearby locations suggests these data can also be used in-
206 terchangeably.

207 Due to the realities of sampling conducted over decades by multiple agencies, sig-
208 nificant interannual, seasonal, depth, and spatial biases are present in the combined data
209 product and must be considered. A detailed description of known biases is provided in
210 Supporting Information S.2; a brief discussion of the ways in which we designed our anal-
211 ysis to minimize these biases in our results follows below. Biases for nutrient data are
212 similar to those for temperature and salinity, and we note that the number of nutrient
213 samples is relatively low compared to the number of hydrographic profiles (Figure S2).
214 As the variables considered herein are frequently not normally distributed, we charac-
215 terize the ‘average’ of a distribution of values using the median rather than the mean,
216 unless otherwise specified.

217 Owing to interannual bias in sampling, which varies by region (Figure S2), our anal-
218 ysis does not include an examination of interannual trends. Rather, we focus on the per-
219 sistence of regional differences over the full duration of the data record. Seasonal bias
220 in sampling is present in all regions due to the difficulty of making measurements dur-
221 ing winter conditions, though this is particularly notable in the QCSt and JS regions (Fig-
222 ure S3). In cases where this seasonal bias is likely to significantly impact our analysis,

223 data are averaged monthly or grouped into summer (May to October) vs. winter (Novem-
224 ber to April) periods.

225 Our analysis examines both the fresh upper and dense lower layer in the two-layer
226 estuarine exchange flow present in much of the study area, necessitating consideration
227 of depth biases in sampling. For consistency between the physical and nutrient data, we
228 calculate the mean value of temperature, salinity, and nutrient concentration data in 25 m
229 bins for most of the analysis. When appropriate, we focus on differences between the ‘up-
230 per’ (<50 m depth) and ‘lower’ (≥ 50 m depth) portions of the water column. The top
231 10 m of T and S profiles are excluded from much of the analysis due to higher uncertainty
232 and the relative scarcity of surface measurements (Supporting Information S.2).

233 To minimize the impacts of spatial biases in sampling on our results, we focus on
234 identifying robust large-scale inter-regional variations. In doing this, we make the im-
235 plicit assumption that variations of water properties within regions (whether captured
236 by our data or not) are smaller than variations between regions. The results herein sup-
237 port this assumption for locations where profiles are available. Nutrient data are spa-
238 tially sparse (Figure S4), and a concerted observational effort would be required to ac-
239 curately quantify smaller-scale spatial variations in nutrient concentrations within each
240 region.

241 We acknowledge that it is not possible to fully eliminate the impacts of sampling
242 bias on our analysis. Our aims are to design our analysis to minimize these impacts to
243 a reasonable extent and to interpret our results within the context of the known biases
244 described above.

245 **3 Results**

246 In what follows, we use the combined data product to quantify regional differences
247 in water properties, which are sustained by the strong tidal mixing in the tidal mixing
248 frontal zone. We examine the spatial and temporal variability of water properties by re-
249 gion, and quantify a spatially-abrupt and temporally-persistent transition within this frontal
250 zone. We show that, despite their geographic proximity, the physical water properties,
251 nutrient ratios, and seasonality in QCSt and JS are distinct from those in the northern
252 SoG and the DI.

3.1 Stratification and inferred tidal mixing strength

While we do not measure ocean currents or mixing directly, we use the stratification in the upper water column as a qualitative proxy to infer the relative strength and delineate the spatial extent of the tidal mixing in each region within the study area. We assume that mixing in this area is primarily tidally-driven based both on previous studies (e.g. Thomson, 1981; Griffin & LeBlond, 1990; Foreman et al., 2004) and on the strong tidal currents present in the JS and DI regions (Figure 1, *Canadian Tide and Current Tables / Tables des marées et courants du Canada* (2019)). We characterize the stratification using the average buoyancy frequency, N^2 , in the upper 50 m of the water column (Figure 2, Supporting Information S.1). Our characterization indicates that the strongest tidal mixing occurs in the DI, where the near-homogenization of the water column is immediately apparent. Relatively weak stratification in the JS region suggests weak tidal mixing there, while relatively strong stratification in QCSt and the SoG suggests minimal or absent tidal mixing in these regions. Regional differences in stratification are similar in summer and winter, with lower values of N^2 overall in winter (Figure S1). Based on these results, we infer that the majority of the tidal mixing occurs in JS and the DI during all seasons. We focus our analysis on regional differences and the transition in properties across the tidal mixing frontal zone (Figure 1), however we note that strong mixing is also known to occur at locations in JS and the DI outside of this zone.

3.2 Temperature and salinity contrast

To investigate how the tidal mixing frontal zone is linked to a transition in water properties, we first examine regional differences in temperature and salinity data (Figure 3). A temperature-salinity (T-S) diagram for JS and the DI (Figure 3, right inset) reveals an abrupt, distinct, and persistent regional contrast in T-S properties, evident in the clear separation between the two regions in T-S space. This abrupt transition between JS and the DI occurs roughly along the 1023 kg m^{-3} isopycnal. Geographically, this transition bisects the study area and the regional differences in properties remain visible in the adjacent regions: temperature and salinity values in QCSt are distinct from those in the SoG (Figure 3, left inset). Specifically, T-S properties in JS are similar to upper ocean waters in QCSt (density $<1025.0 \text{ kg m}^{-3}$), while properties in the DI resemble those of upper ocean waters in the SoG (density $<1023.0 \text{ kg m}^{-3}$) (Figure 3 insets, density contours). The QCSt/JS regions have T-S properties that more closely re-

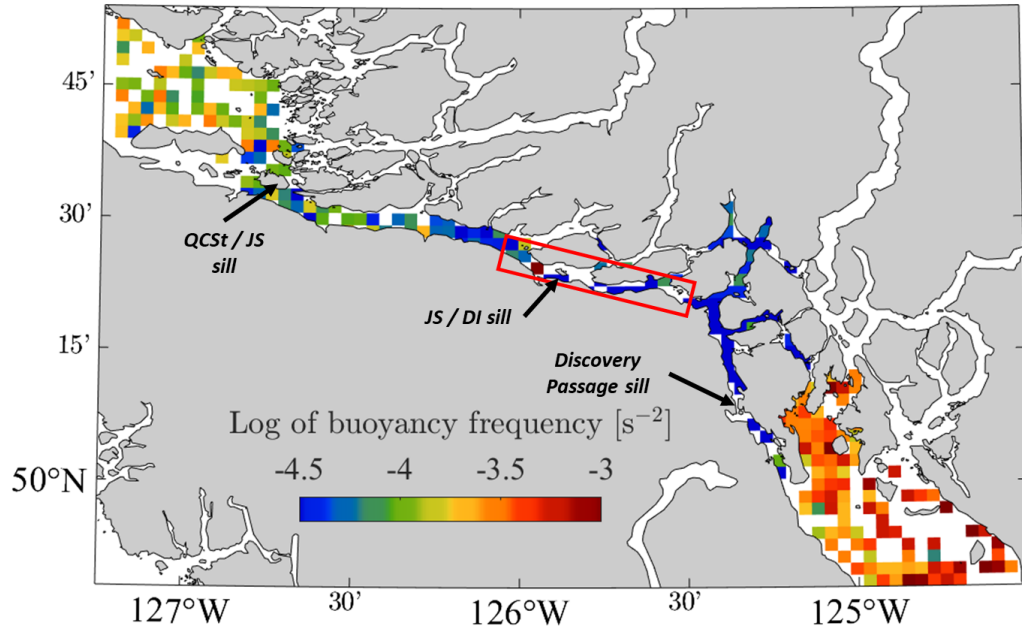


Figure 2. Log of buoyancy frequency, N^2 (in s^{-2}), in the upper 50 m of the water column, calculated from 2 m vertically-binned temperature and salinity profile data, with the median value for May to October shown. Within each 2.5 km square grid box, a median value for each month is calculated, then the median value of the summer months is determined. White grid boxes are locations with no data available, or outside the study area. Winter months (Figure S1) display similar regional differences but lower stratification overall. The approximate locations of shallow sills mentioned in the text are indicated, as is the tidal mixing frontal zone (red box).

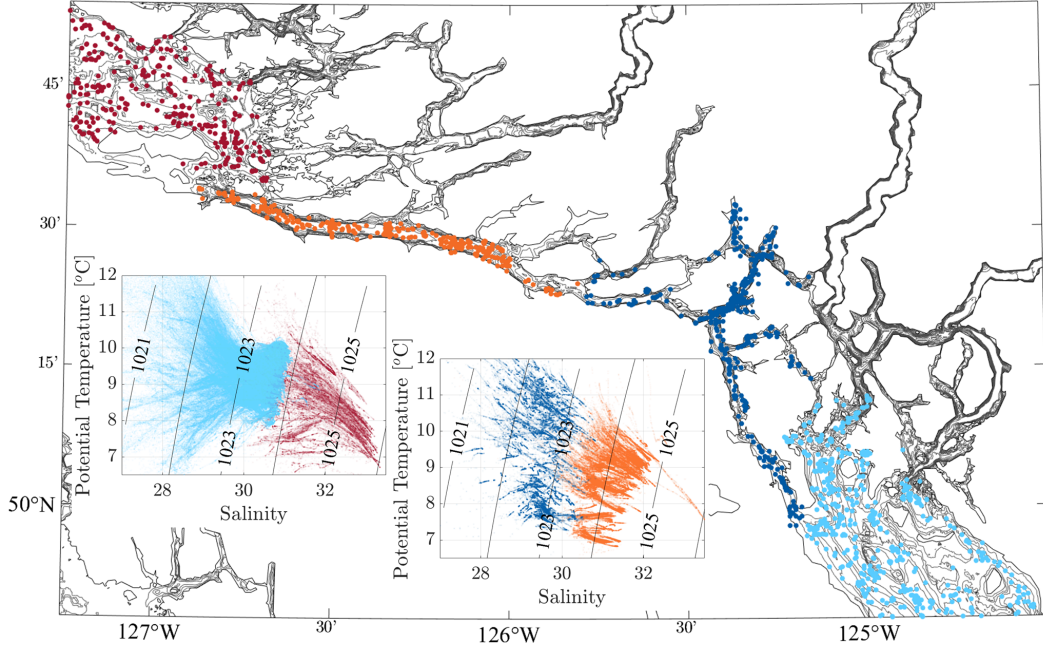


Figure 3. (Map) Locations of hydrographic profiles coloured by region, with QCSt in red, JS in orange, the DI in dark blue and the SoG in light blue. (Insets) Temperature-salinity diagrams for all potential temperature and salinity profile data from the locations on the map, coloured by region. Data have not been binned or averaged. Black lines give contours of potential density.

285 semble values seen in the open Northeast Pacific Ocean adjacent to the BC continen-
 286 tal shelf (e.g. Thomson & Krassovski, 2010), whereas the SoG/DI regions are warmer
 287 and fresher year-round. The relatively cooler and more saline waters in QCSt and JS re-
 288 lative to the SoG and DI may thus reflect their proximity and higher connectivity to the
 289 open ocean.

290 An examination of the average seasonal cycles in the upper (10-50 m depth) and
 291 lower (50-200 m depth) water column (Figure 4) allows us to assess seasonal variabil-
 292 ity in this regional T-S contrast. Regional differences in salinity are roughly constant year-
 293 round in the upper water column (Figure 4a). In contrast, there is a summer increase
 294 in salinity in the lower water column (Figure 4b) seen only in QCSt and JS caused by
 295 seasonal upwelling, discussed in Section 3.4. In the upper water column, the median salin-
 296 ity in the SoG is 2.2 units fresher than in QCSt, while median salinity in the DI region
 297 is 1.4 units fresher than in JS. The largest regional difference in the upper water column
 298 occurs in August, when the SoG and DI are 2.6 units fresher than QCSt. In the lower

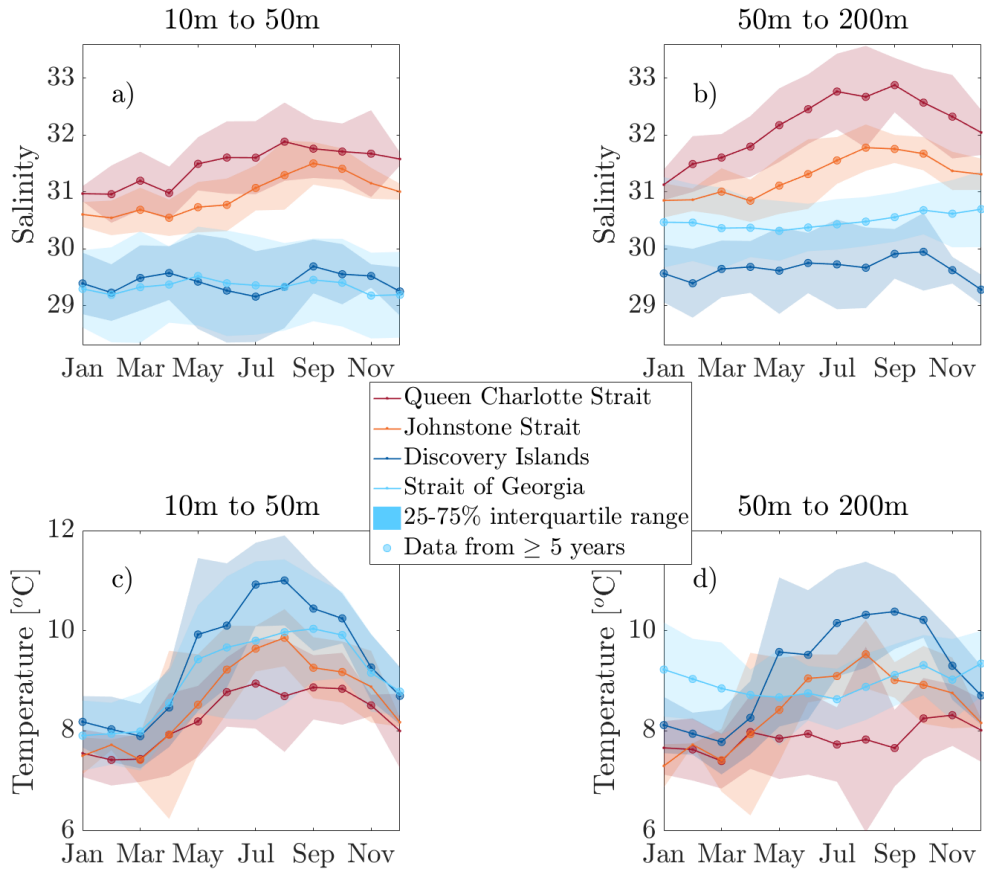


Figure 4. A comparison of regional seasonal cycles in a) salinity from 10-50 m depth, b) salinity from 50-200 m depth, c) potential temperature from 10-50 m depth, and d) potential temperature from 50-200 m depth. Lines give median monthly values for data from all available years with dots indicating months with data from 5 or more years. Shaded envelopes give the 25-75% interquartile range. Colour corresponds to region as indicated in the legend.

299 water column, median salinity in the SoG is 1.9 units fresher than in QCSt, and median
 300 salinity in the DI region is 1.5 units fresher than JS. The largest regional difference oc-
 301 curs in July, when the DI is 3.0 units fresher than QCSt. The reduced salinity contrast
 302 between the upper and lower water column in JS and the DI region, relative to that in
 303 the SoG and QCSt, is likely due to homogenization of the deep waters with the overly-
 304 ing surface layers through strong tidal mixing. Consistent with this picture, the fresh-
 305 est and warmest deep waters are in the DI, where the strongest tidal mixing occurs.

306 Regional temperature differences are also present year-round. The magnitude of
 307 the temperature contrast between regions varies seasonally in both the upper and lower
 308 portions of the water column. In the upper water column (Figure 4c), temperatures in
 309 summer (May to October) in the SoG and DI are often 1-2°C warmer than in QCSt and
 310 JS, though variations between months are large. The largest regional difference occurs
 311 in August, when the DI is 2.3°C warmer than QCSt. Regional temperature differences
 312 in the upper water column in winter (November to April) are generally much smaller (typ-
 313 ically less than 1°C), reflecting the influence of large-scale atmospheric conditions that
 314 span the study area as a whole. In the lower water column (Figure 4d), temperatures
 315 in the SoG and QCSt display less seasonal variation, with temperatures in the SoG roughly
 316 1°C warmer than QCSt year-round. In contrast, JS and the DI show a pronounced sea-
 317 sonal cycle matching that in the upper water column. The largest regional difference oc-
 318 curs in September, when the DI is 2.7°C warmer than QCSt. Minimal variation in tem-
 319 perature between the upper and lower water column in JS and the DI is likely due to
 320 the strong vertical mixing characteristic of these regions.

321 **3.3 Density contrast**

322 In BC coastal waters, density is primarily but not solely controlled by salinity, and
 323 so displays a persistent lateral gradient similar to that in salinity within the regions of
 324 strongest tidal mixing. The temperature and salinity contrasts detailed above result in
 325 ranges of potential density values in QCSt and JS that rarely overlap with those observed
 326 in the SoG and DI, in both the upper (10-50 m depth) and lower (≥ 50 m depth) water
 327 column (Figure 5). The densest water is found deep in QCSt, and the lightest at the sur-
 328 face in the SoG. The lightest water in QCSt (JS) is denser than the densest water in the
 329 SoG (DI) for the large majority of observations. The density distributions in JS vs. the
 330 DI and in QCSt vs. the SoG thus have minimal overlap and are statistically distinct at

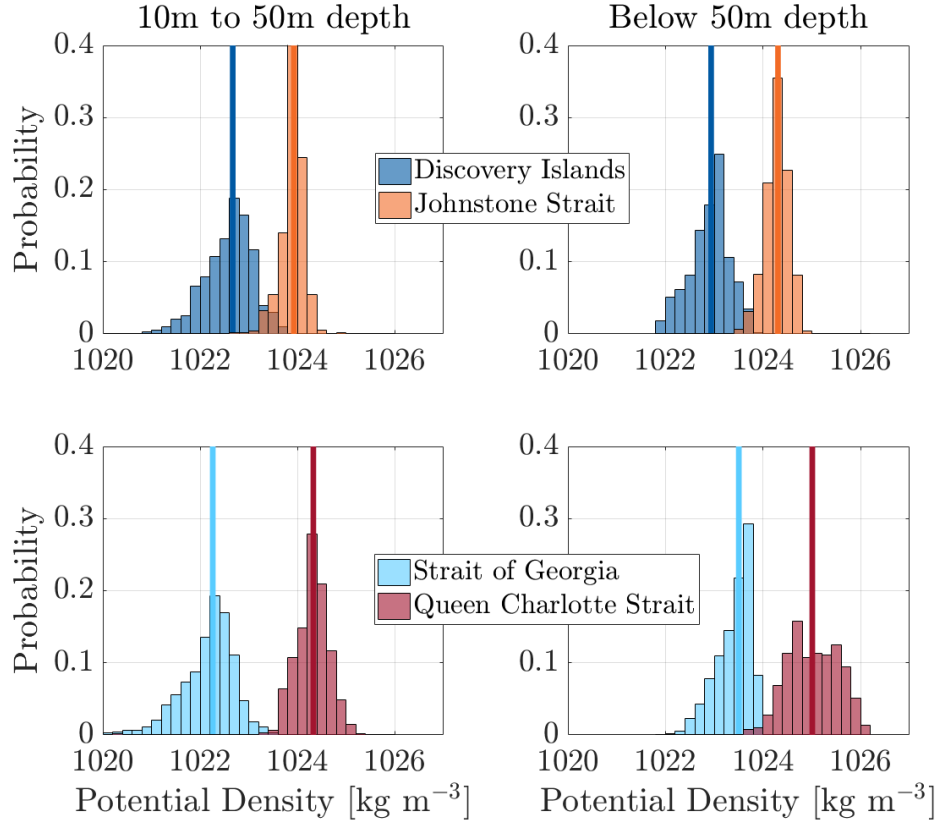


Figure 5. Regional distributions of potential density calculated using the full temperature and salinity dataset, binned every 25 m in the vertical, for the upper 10-50 m depth of the water column (left) and below 50 m depth (right). Vertical lines give the median value of density in each distribution.

331 the 99% confidence level ($p < 0.001$) using a Kolmogorov-Smirnov test (“Kolmogorov–Smirnov
 332 Test”, 2008), which is used to determine the likelihood that two separate distributions
 333 of data are drawn from the same overall distribution.

334 The inclusion of year-round temperature and salinity profile data spanning 1932
 335 to 2018 demonstrates that this transition in density persists between seasons and inter-
 336 annually, for all months and for the 70 individual years for which data are available. An
 337 examination of near full-depth profile data confirms that these properties change rapidly
 338 in the horizontal at all subsurface depths (see Section 4.1 for further details). Addition-
 339 ally, this transition is present during both the spring and neap phases of the fortnightly
 340 tidal cycle. To confirm that both spring and neap tides are well-sampled in all regions,
 341 we note that samples are collected with weekly or higher frequency for 39% of days sam-

	QCSt	JS	DI	SoG
	Nutrient concentration ($\mu\text{mol L}^{-1}$)			
Nitrate	23 ± 6	23 ± 5	25 ± 4	29 ± 5
Phosphate	1.9 ± 0.5	1.9 ± 0.4	2.2 ± 0.3	2.5 ± 0.4
Silicate	38 ± 14	39 ± 12	49 ± 9	54 ± 10
	Nutrient molar ratio			
N:P	12.3 ± 0.8	12.2 ± 1.0	11.4 ± 1.1	11.3 ± 1.0
N:Si	0.59 ± 0.08	0.58 ± 0.06	0.51 ± 0.03	0.51 ± 0.06
P:Si	0.048 ± 0.005	0.048 ± 0.005	0.045 ± 0.005	0.045 ± 0.005

Table 1. Median values and the 25-75% interquartile ranges for full-depth nutrient concentrations and nutrient molar ratios in each region. The median and interquartile range are given, rather than the mean and standard deviation, as the data are not normally distributed. For comparison, Redfield-Brzezinski values are 16 for N:P, 1.1 for N:Si, and 0.07 for P:Si.

342 pled in QCSt, 54% in JS, 34% in the DI, and 66% in the SoG. Full-depth density pro-
343 files on either side of the tidal mixing frontal zone have no notable differences during spring
344 vs. neap tides (not shown). This lack of evidence for significant spring-neap modulation
345 of the density structure across the tidal mixing frontal zone is significant. Spring-neap
346 modulation of the residual circulation is a well-known indicator of tidal mixing (Hibiya
347 & LeBlond, 1993; Park & Kuo, 1996; MacCready et al., 2018), and its apparent absence
348 here suggests that the strength and spatial extent of the tidal mixing may be sufficient
349 to permanently disrupt the two-layer estuarine exchange flow within the tidal mixing frontal
350 zone (tidal currents remain above 75 cm s^{-1} at some locations in the DI even during low
351 neap tides). However, more measurements within the tidal mixing frontal zone would
352 be needed to fully analyze tidal modulation of the mixing front.

353 **3.4 Contrast in nutrient molar ratios**

354 In addition to the regional separation in physical water properties, there are sta-
355 tistically significant differences in nutrient molar ratios between the QCSt/JS and SoG/DI
356 regions. Regional distributions of the molar ratio of nitrate to phosphate (Figure 6), ni-
357 trate to silicate (Figure 7), and phosphate to silicate (Figure 8) are examined for both
358 the upper ($<50 \text{ m}$ depth) and lower ($\geq 50 \text{ m}$ depth) water column. Median values and
359 interquartile ranges for nutrient concentrations and nutrient molar ratios for each region

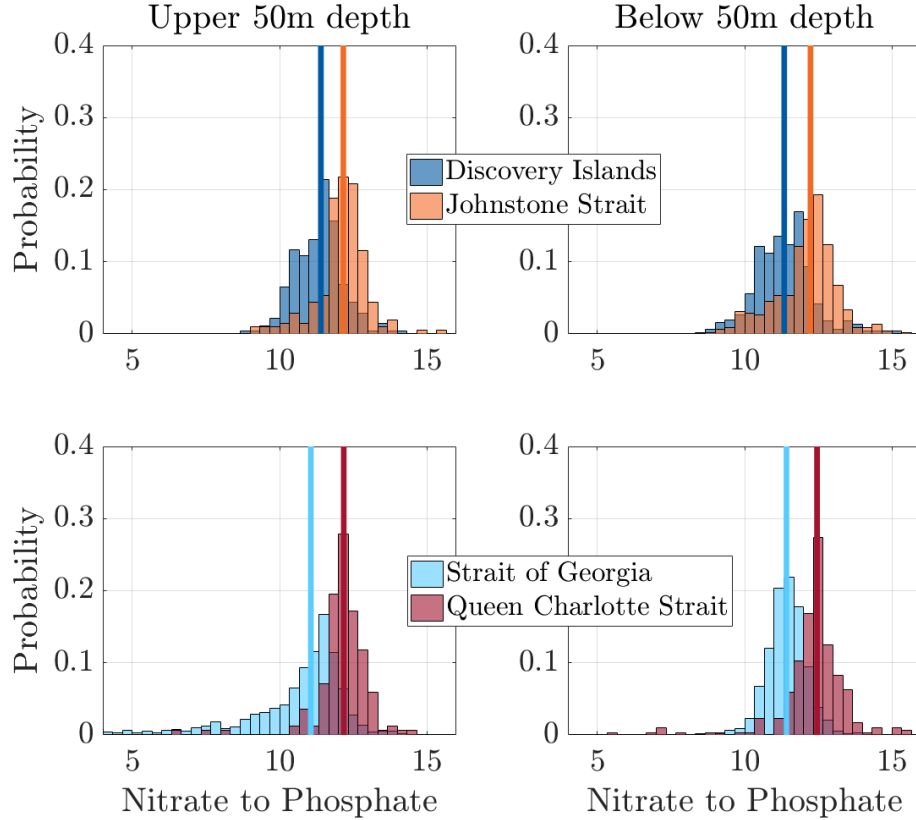


Figure 6. Regional distributions of the nitrate to phosphate molar ratio, calculated using the full nutrient dataset, binned every 25 m in the vertical, for the upper 50 m depth of the water column (left) and below 50 m depth (right). Vertical lines give the median value for each distribution.

360 are given in Table 1. Nutrient ratios are assessed relative to the Redfield-Brzezinski mo-
 361 lar ratios for carbon to silicon to nitrogen to phosphorus (Brzezinski, 1985), which are
 362 canonically C:Si:N:P = 106:15:16:1 in open-ocean waters. Our nutrient ratios are gen-
 363 erally lower in all regions than these canonical open-ocean values (Table 1). Median val-
 364 ues of the nutrient ratios in both the upper and lower water column are closest to canon-
 365 ical open-ocean values in QCSt and JS, and differ most significantly from canonical open-
 366 ocean values in the SoG and DI.

367 Median values for the molar ratio of nitrate to phosphate (N:P, Figure 6) vary from
 368 11.3 in the SoG to 12.3 in QCSt (Table 1), an 8% difference. The largest regional dif-
 369 ference is for the nitrate to silicate ratio (N:Si, Figure 7), with a 14% difference between
 370 the median value of 0.59 in QCSt and 0.51 in the SoG and DI (Table 1). The phosphate

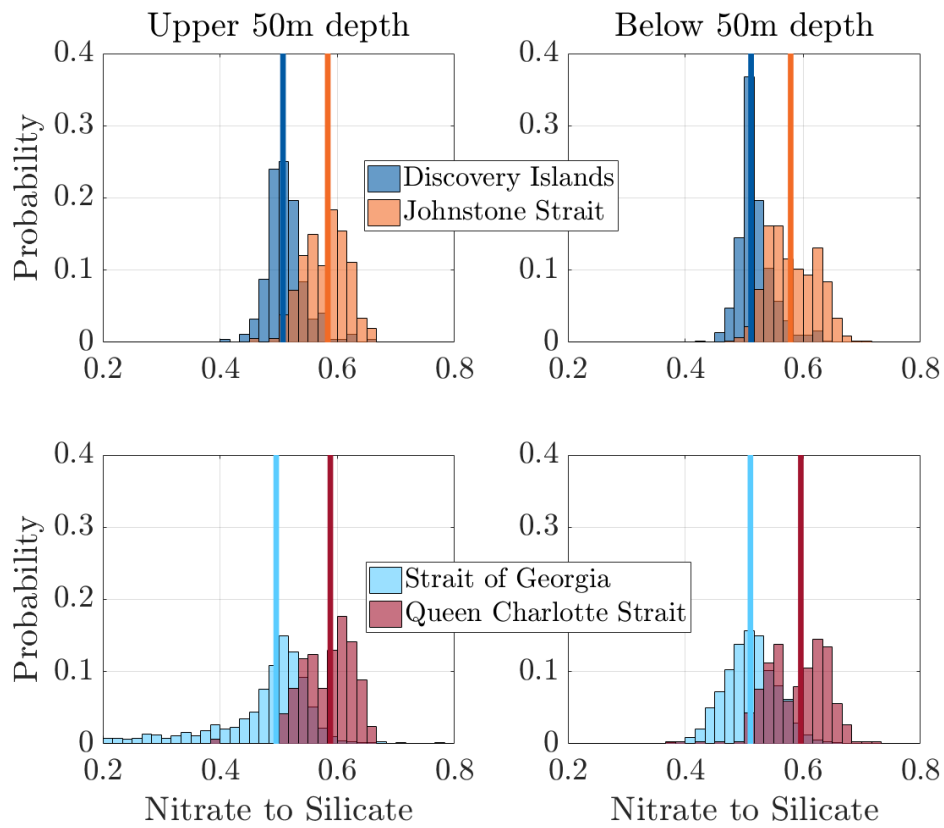


Figure 7. As in Figure 6, but for the molar ratio of nitrate to silicate.

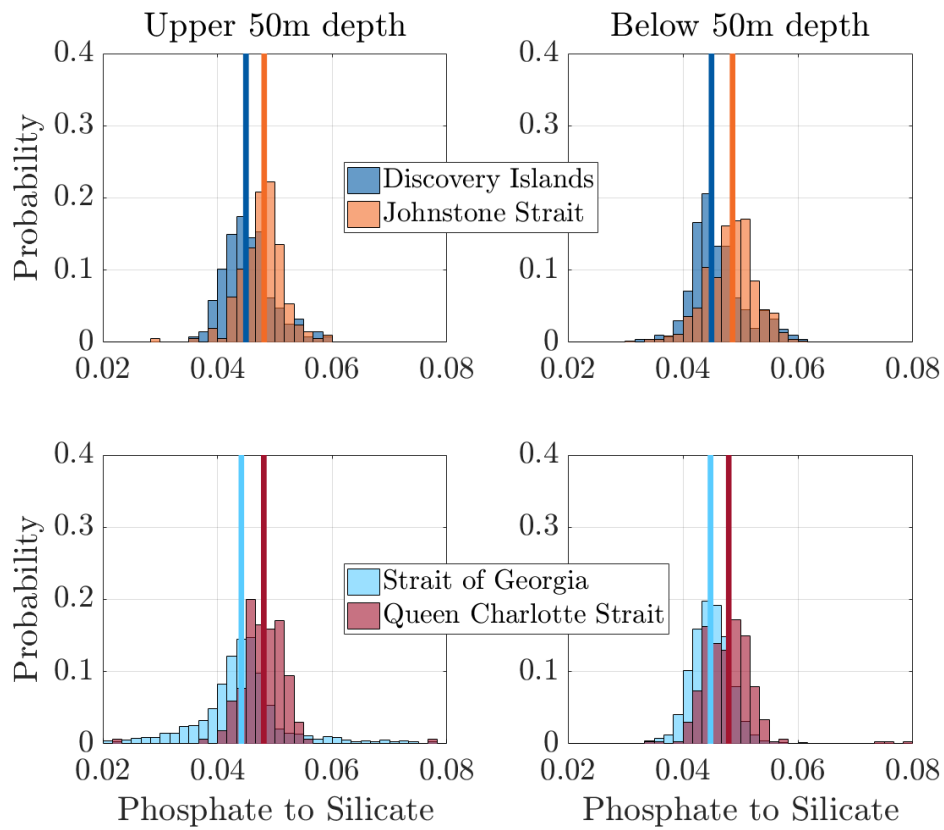


Figure 8. As in Figure 6, but for the molar ratio of phosphate to silicate.

371 to silicate ratio has the smallest regional variation (P:Si, Figure 8), with a 7% difference
372 in median value between 0.048 in QCSt/JS and 0.045 in the SoG/DI (Table 1). Distri-
373 butions of all three nutrient molar ratios in QCSt and JS are statistically distinct from
374 those in the SoG and DI at the 99% confidence interval ($p < 0.001$ for all three ratios) based
375 on a Kolmogorov-Smirnov test, in both the upper and lower water column.

376 Nutrient ratios vary regionally as a result of relative differences in nutrient concen-
377 tration (Table 1, Supporting Information S.3). Median nutrient concentrations are low-
378 est in QCSt and highest in the SoG, with relatively high silicate concentrations in the
379 SoG contributing significantly to regional differences. Nutrient ratio distributions in the
380 upper water column in the SoG have long tails (Figures 6, 7, 8), evidence of occasional
381 nitrate and/or phosphate depletion (Masson & Peña, 2009), which is common in coastal
382 waters particularly in the late summer (Howarth & Marino, 2006). However, nutrient
383 concentrations in all regions are rarely limiting (Table 1, Supporting Information S.3).
384 In addition to differing degrees of nutrient depletion by biology, other possible causes for
385 the regional differences in nutrient ratios are differences in source waters or transport
386 pathways for nutrient input, as discussed further in Section 4.2.

387 3.5 Seasonal upwelling

388 Closer examination of the seasonal cycle of physical water properties and nutrient
389 ratios in the deep waters of QCSt and the SoG reveals differences in the timing and mag-
390 nitude of upwelled water arriving from the Northeast Pacific Ocean. (Seasonal variations
391 in deep water properties in JS and the DI are suppressed due to tidal mixing, but are
392 otherwise qualitatively similar to those in QCSt and the SoG respectively.) In the lower
393 water column in QCSt, water upwelled from the deep Northeast Pacific causes decreased
394 temperatures (Figure 4d), increased salinity (Figure 4b), increased density (Figure 9a),
395 and increased nutrient concentrations (Figure 9b) beginning in April and peaking in Au-
396 gust. By contrast, upwelled water in the SoG region is associated with only minor vari-
397 ations in the seasonal cycle of these properties, likely due to significant modification in
398 Haro Strait before its arrival in the northern Strait of Georgia (LeBlond et al., 1991; Mackas
399 & Harrison, 1997). Here, a small seasonal increase in deep salinity (Figure 4b) and den-
400 sity (Figure 9a) reaches a maximum in October/November, with no accompanying in-
401 crease in nutrient concentration or decrease in temperature (these attain their maximum
402 and minimum values, respectively, in July). These differences in seasonal cycle magni-

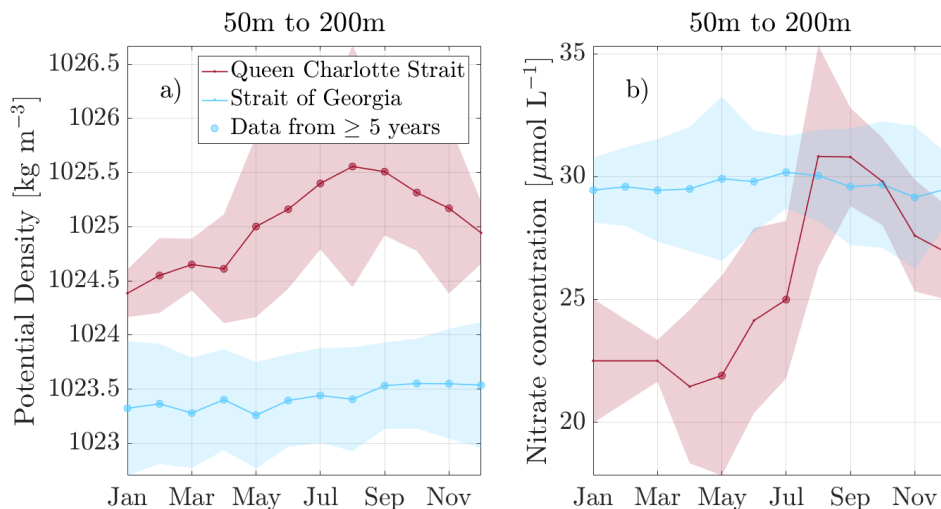


Figure 9. a) Potential density and b) nitrate concentration by month for the lower water column (50-200 m) in Queen Charlotte Strait (red) and the Strait of Georgia (light blue). Lines give the monthly median density and nitrate values, with large dots indicating at data from at least five years. Shading gives the 25-75% interquartile range.

403 tude and the timing of the arrival of upwelled water in QCSt/JS vs. the SoG/DI regions
 404 are significant because they suggest distinct transport pathways for upwelled water (we
 405 suggest these pathways are to the north of Vancouver Island for QCSt/JS and to the south
 406 through the Strait of Juan de Fuca for the SoG/DI), with little to no exchange of deep
 407 water through the tidal mixing frontal zone. These differences in the seasonality of deep
 408 water properties between regions adds further support to the emerging picture of QCSt/JS
 409 and the SoG/DI as separate environments, largely isolated from each other, and likely
 410 to respond differently to changes in large-scale open-ocean forcing.

411 **4 Discussion**

412 The observed regional differences in physical and biogeochemical properties reported
 413 herein are consistent with an effective disruption of the two-layer estuarine exchange flow
 414 between QCSt and the SoG due to tidal mixing. Here we address, first, possible impli-
 415 cations for circulation, and second, some direct and indirect effects on marine ecosys-
 416 tems in the study area.

4.1 Tidal mixing and circulation

A visualization of the average density structure along a transect connecting eastern QCSt to the northern SoG during upwelling favorable conditions (Figure 10) shows a strong lateral density gradient between JS and the DI. The abrupt transition between these regions in the tidal mixing frontal zone is visible as near-vertical isopycnal structure, indicating homogenization of the water column, for a narrow range of densities around 1023 kg m^{-3} (Figure 10; $\sim 200 \text{ km}$). As demonstrated in Section 3.3, waters in JS are almost completely separate in density space from waters in the DI at all depths below the near-surface ($< 10 \text{ m}$). Only very near the surface do we see evidence of freshwater advection from the DI into JS, a signal which is likely caused by wind forcing dominating the direction of surface currents there (Chandler et al., 2017). Although the scarcity of data in the tidal mixing frontal zone precludes identifying the exact number and location of individual density fronts, we estimate that the lateral gradient between regions spans a distance of at least $\sim 75 \text{ km}$ within the narrow, shallow channels of JS and the DI (Figure 10; $\sim 150\text{-}225 \text{ km}$). Vigorous tidal mixing has been reported both within the tidal mixing frontal zone and in adjacent channels; Thomson1981 mentions particularly strong tidal mixing over the Discovery Passage sill (Figure 10; $\sim 275 \text{ km}$). The relatively shallow sills between regions also affect the density structure in the study area. The densest waters in QCSt are isolated from JS by the $< 100 \text{ m}$ deep sill at $\sim 100 \text{ km}$ along the transect. Similarly, the $< 100 \text{ m}$ deep Discovery Passage sill prevents dense deep waters in the SoG from entering the DI. In combination, these factors produce the dramatic lateral density gradient between the QCSt/JS and SoG/DI regions.

Although details of the circulation within our study area are not well-known, the abrupt and persistent transition in density and other water properties that we document is consistent with limited exchange between the QCSt/JS and SoG/DI regions in all subsurface waters (i.e. $> 10 \text{ m}$). Rather than the strong two-layer estuarine exchange flow typical of stratified estuaries, transport through the tidal mixing frontal zone is likely to occur via a weak residual one-way flow from the DI towards JS, similar to that observed in a well-mixed estuary (e.g. MacCready & Geyer, 2010). In such a case where the horizontal advection is reduced, the primary transport of properties through the tidal mixing frontal zone must occur via mixing, operating more slowly over smaller spatial scales (MacCready et al., 2018). The inhibition of horizontal transport is additionally expected to cause recirculation of much of the inflowing water (Griffin & LeBlond, 1990;

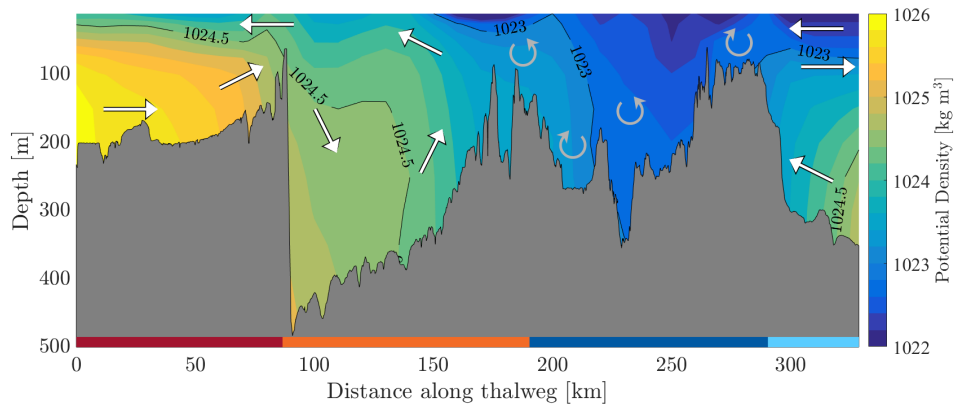


Figure 10. Lateral transect of potential density following the thalweg (line of deepest bathymetry) from QCSt to the SoG during mid-summer (June to August) using data from all available years. Data are binned every 10 km in the horizontal, and every 25 m in the vertical to 100 m depth, then every 50 m to 500 m depth (due to a paucity of full-depth profiles). Black contours show select isopycnals as indicated. Coloured bars along the x-axis give the boundaries of the four regions as shown in Figure 1. Data in the very near-surface waters (<10 m depth) have been excluded. White arrows show the hypothesized recirculation and transport pathways of inflowing water from QCSt into JS and from the SoG into the DI respectively. Gray arrows indicate the region of strong mixing in the tidal mixing frontal zone and Discovery Passage.

450 Hibiya & LeBlond, 1993; Park & Kuo, 1996; MacCready, 1999). Based on these consid-
 451 erations, we propose a hypothetical circulation pattern consistent with our results and
 452 past studies of circulation in the study area. This circulation is illustrated schematically
 453 for upwelling favorable conditions in Figure 10. Below the very near-surface, our results
 454 suggest that a significant fraction of the water entering JS from QCSt is recirculated back
 455 out to QCSt. Similarly our results suggest that a significant proportion of water enter-
 456 ing the DI from the SoG is recirculated back to the SoG. While the visualization in Fig-
 457 ure 10 is specific to the months of June to August, our results demonstrate that the tran-
 458 sition in properties across the tidal mixing frontal zone persists year-round (Section 3.2),
 459 suggesting that these recirculations driven by tidal mixing occur regardless of season.

460 We further suggest likely transport pathways for the inflowing water on either side
 461 of the tidal mixing frontal zone (Figure 10). We hypothesize that during summer dense
 462 upwelled water flows from QCSt over the sill into the deep JS basin, is mixed vertically
 463 within the tidal mixing frontal zone, and passes back out to QCSt near the surface. This
 464 circulation in JS is similar to that in other deep basins situated between shallow sills,
 465 such as the main basin in nearby Puget Sound (Ebbesmeyer & Barnes, 1980), and shares
 466 similarities with partially-mixed (moderately-stratified) estuaries (MacCready & Geyer,
 467 2010) with fresh water from the DI playing the role of river inflow at the head of the es-
 468 tuary. On the other side of the tidal mixing frontal zone, we hypothesize that water from
 469 the SoG enters Discovery Passage in the DI primarily above ~ 100 m depth, is mixed ver-
 470 tically with denser water intermittently sourced from the SoG, and passes back out to
 471 the SoG at mid-depth (>100 m on average, Thomson (1981)). These proposed trans-
 472 port pathways are consistent with the similarity in water properties observed between
 473 JS and the upper 30-50 m of QCSt (<1025 kg m $^{-3}$), the similarity in properties observed
 474 between the SoG and DI in the upper ~ 80 m (<1023 kg m $^{-3}$), the predictions of regional
 475 models (Foreman et al., 2006, 2012; Khangaonkar et al., 2017; Olson et al., 2020), and
 476 current meter records in JS (Thomson & Huggett, 1980) and Discovery Passage (Foreman
 477 et al., 2012).

478 Although it is not surprising that QCSt and the SoG have different water prop-
 479 erties, as the latter is an inland sea while the former opens directly to the continental
 480 shelf and Northeast Pacific Ocean, conventional wisdom has held that waters from the
 481 SoG are advected through the DI and JS into QCSt and vice-versa (e.g. Godin et al.,
 482 1981) driving a significant exchange of properties. Our results and hypothesized circu-

483 lation suggest that a more accurate view of the QCSt/JS and SoG/DI regions are as dis-
484 tinct, largely isolated marine environments, with different physical water properties, sea-
485 sonality, connectivity to the open ocean, and pathways of nutrient delivery. An impor-
486 tant implication of this is that we expect regional responses to stressors to differ, par-
487 ticularly for stressors originating in the open ocean.

488 As an example of differing regional responses to a stressor, we briefly examine the
489 effect of the marine heatwave known as The Blob on temperatures in the QCSt/JS and
490 SoG/DI regions (Figure 11). This heatwave and a subsequent El Niño impinged on BC
491 coastal waters beginning in 2014 (Bond et al., 2015), with a subsurface expression af-
492 fecting coastal waters through at least 2018 (Jackson et al., 2018). We compare distri-
493 butions of temperature in the upper water column pre-2014 vs. during the Blob years
494 in the QCSt/JS vs. SoG/DI regions. The anomalous heat associated with this heatwave
495 is visible on both sides of the tidal mixing frontal zone, however the effects of the heat-
496 wave are more pronounced in QCSt/JS, presumably due to its higher connectivity with
497 the open ocean. In particular, the temperature anomaly associated with the heatwave
498 is larger in QCSt/JS; the median of the temperature distribution shifts upward by 0.81°C
499 (compared to 0.66°C in the SoG/DI). In addition, there is a complete loss of the cold-
500 est waters in QCSt/JS, which is not observed on the SoG/DI side of the tidal mixing frontal
501 zone. In contrast, the SoG/DI region experiences little change in the range of temper-
502 atures observed, though cold temperatures become more rare and warm temperatures
503 more common.

504 **4.2 Implications for ecosystems**

505 Tidal mixing has important direct and indirect implications for ecosystems. First,
506 we consider the direct role of tidal mixing in vertical nutrient transport and light avail-
507 ability. Our results show the arrival of upwelled water in JS in summer (Figure 4), and
508 we hypothesize that strong tidal mixing and recirculation (Figure 10) acts to bring deep
509 nutrients to the surface, which then exit into the more strongly-stratified waters of QCSt.
510 On the other side of the tidal mixing frontal zone, these dynamics result in nutrient-rich
511 water re-entering the SoG at mid-depth in the Discovery Passage plume (e.g. Olson et
512 al., 2020) and help fuel phytoplankton blooms in the SoG (Del Bel Belluz et al., 2020).
513 Despite high near-surface nutrient concentrations (Table 1), the weakly-stratified waters
514 of JS and the DI are themselves regions of low primary productivity (Mahara et al., 2020).

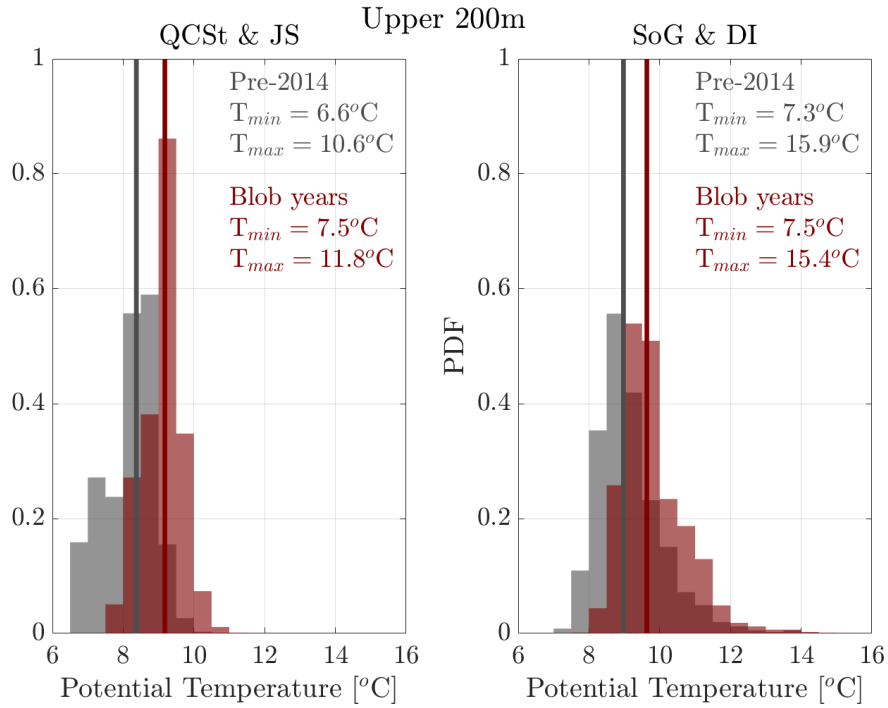


Figure 11. Distributions of potential temperature from 10-200 m depth for years when the marine heatwave known as The Blob affected coastal waters (dark red) and for years prior to this event (gray) in QCSt/JS (left) and in the SoG/DI (right). Vertical lines give the median of each distribution. Data used are binned every 25 m in the vertical. Data from Jan-Mar are excluded as no samples are available in QCSt during those months for 2014-onwards. Minimum and maximum temperatures for the two periods are as given.

515 These high-nutrient, low-productivity conditions are attributed to full-depth tidal mix-
516 ing limiting the light available to phytoplankton for growth (Masson & Peña, 2009; McK-
517 innell et al., 2014; Murray et al., 2015). The resulting low primary productivity is known
518 to have wider ecosystem effects, with migrating juvenile salmon experiencing poor for-
519 aging success in JS and the DI (James et al., 2020). However, our results suggest that
520 while tidal mixing in JS and the DI limits productivity within those regions, it may si-
521 multaneously enhance and sustain the overall high levels of productivity observed in QCSt
522 and the SoG.

523 An important implication of the differing transport pathways resulting from the
524 recirculation of inflowing water caused by tidal mixing is that the primary sources of nutrient-
525 rich waters supplying QCSt and the SoG likely differ. This may explain the observed re-
526 gional differences in nutrient molar ratios (Figures 6, 7, 8). Seasonal upwelling appears
527 to be the dominant source of nutrient replenishment in QCSt/JS, with upwelled water
528 arriving from the open ocean via Queen Charlotte Sound. Consistent with this picture,
529 nutrient ratios in QCSt/JS are closer to ideal Redfield-Brzezinski values, which describe
530 ratios typical of open-ocean conditions (Brzezinski, 1985). By contrast, nutrient ratios
531 in the SoG/DI are further from these ideal values, as expected for coastal waters with
532 major inputs of silicate from freshwater runoff (Whitney et al., 2005) and accumulation
533 of nutrients through remineralization in SoG waters with high residence time (Pawlowicz
534 et al., 2007; Sutton et al., 2013). As such, while nutrient cycling in QCSt/JS is likely to
535 be directly impacted by changes in the volume or properties of upwelled water, the SoG/DI
536 region is likely more susceptible to changes in terrestrial and river inputs or in-situ wa-
537 ter properties that affect remineralization in the water column and sediments.

538 Differences in oceanic nutrient ratios provide more than a measure of nutrient lim-
539 itation; regional differences in nutrient ratios are expected to influence the species com-
540 position of phytoplankton communities and their cellular stoichiometry (Geider & La Roche,
541 2002; Arrigo, 2005; Klausmeier et al., 2008). Although nutrients are typically plentiful
542 across the study area (Section 3.4, Supporting Information S.3), nutrient molar ratios
543 have the potential to limit the productivity of some phytoplankton species. For exam-
544 ple, in QCSt where ratios are most similar to open-ocean values, we might expect phy-
545 toplankton communities to share similarities with nearby open-ocean or continental shelf
546 communities. In the SoG, where ratios are further from the ideal Redfield-Brzezinski val-
547 ues, we might expect significant differences in species composition. This is an area of ac-

548 tive research, and indeed, cross-shelf differences in phytoplankton community compo-
549 sition and size structure in response to changing nutrient ratios have been demonstrated
550 in Alaska (Strom et al., 2006). Phytoplankton species composition and prevalence can
551 in turn affect the quantity and nutritional quality of their zooplankton grazers (El-Sabaawi
552 et al., 2009; Costalago et al., 2020), with implications for the next trophic level, includ-
553 ing juvenile salmon and forage fish (e.g. Pacific herring) (Litzow et al., 2006; Godefroid
554 et al., 2019; James et al., 2020). The tidal mixing and its hypothesized effects on circu-
555 lation therefore impact not only levels of primary productivity via nutrient transport,
556 but also potentially underlie certain regional ecosystem differences within the study area.

557 **5 Summary**

558 Using a combined DFO, UBC, and Hakai Institute data product, we document a
559 spatially-abrupt and temporally-persistent transition in physical water properties and
560 nutrient ratios bisecting our study area in British Columbia coastal waters. The tran-
561 sition occurs in the weakly-stratified channels of the eastern Discovery Islands and John-
562 stone Strait, between Queen Charlotte Strait and the Strait of Georgia, where strong tidal
563 mixing appears to disrupt the two-layer estuarine exchange flow and drive recirculations
564 of inflowing water. We quantify an abrupt change in salinity and temperature across this
565 ‘tidal mixing frontal zone’, with properties in Queen Charlotte Strait and Johnstone Strait
566 more closely resembling cool and saline open-ocean conditions in all seasons and more
567 strongly influenced by the summer arrival of dense, cold, nutrient-rich water upwelled
568 from the Northeast Pacific Ocean. We identify a dramatic lateral gradient in density, pre-
569 viously described by Thomson (1976, 1981), and show that it spans the full depth of the
570 water column and persists year-round for the duration of the multi-decadal data record.
571 We find that distributions of nutrient molar ratios in Queen Charlotte Strait and John-
572 stone Strait are statistically distinct from those in the northern Strait of Georgia and
573 Discovery Islands, and are closer to ideal open-ocean Redfield-Brzezinski values.

574 The ‘tidal mixing frontal zone’ provides an ideal case study for the ability of strong,
575 sustained tidal mixing to maintain regional differences in water properties. Despite lack-
576 ing direct measurements of circulation, our results suggest limited exchange of water through
577 the region of strongest tidal mixing. As such, Queen Charlotte Strait and the Strait of
578 Georgia appear largely isolated from each other and are shown to respond differently to
579 environmental stressors such as marine heatwaves. Furthermore, significant regional dif-

580 ferences in marine environmental conditions and nutrient transport pathways, such as
581 those observed within the study area, are expected to influence both the quantity and
582 quality of primary production available to higher trophic levels. Our results demonstrate
583 the degree to which tidal mixing can result in such regionalization, and may be broadly
584 relevant to other highly productive coastal habitats such as those found in Alaska and
585 on the southwest coasts of Chile, New Zealand, and Scandinavia.

586 **Acknowledgments**

587 Data collected by DFO and UBC and used in this study are archived and publicly avail-
588 able at cioospacific.ca and at waterproperties.ca. The data collected by DFO are also
589 accessible through the Institute of Ocean Sciences Data Archive, Ocean Sciences Divi-
590 sion, Department of Fisheries and Oceans Canada at [www.pac.dfo-mpo.gc.ca/science/oceans/data-](http://www.pac.dfo-mpo.gc.ca/science/oceans/data-donnees/index-eng.html)
591 [donnees/index-eng.html](http://www.pac.dfo-mpo.gc.ca/science/oceans/data-donnees/index-eng.html). Data collected by the Hakai Institute are available at hecate.hakai.org.
592 We thank the many scientists, students, technicians, and crew from the Pacific Biolog-
593 ical Station, the Institution of Ocean Sciences, the University of British Columbia, and
594 the Hakai Institute whose collective efforts to sample and understand the BC coastal ocean
595 over the last 90 years have provided us with the observations and past research that made
596 this work possible. We are particularly grateful for the efforts of Rick Thomson who pi-
597 oneered much of the research in the Johnstone Strait region. We also specifically acknowl-
598 edge the field crews at the Hakai Institute's Quadra Island field station and Salmon Coast
599 Field Station for their time and energy in the field collection and curation of oceanographic
600 data.

601 This research was conducted as part of the Hakai Institute's Juvenile Salmon Pro-
602 gram, funded by the Tula Foundation. H. Dosser received funding from the Tula-Mitacs
603 Canada Grants IT09911 through internships No. FR23012, FR23020, and FR23028 and
604 through a Marine Environmental Observation, Prediction and Response Network (MEOPAR)
605 - Networks of Centres of Excellence (NCE) Postdoctoral Fellowship Award. B. Hunt and
606 J. Jackson were funded by the Tula Foundation. S. Waterman was supported by MEOPAR
607 - NCE and Ocean Networks Canada through Early Career Faculty Grant 2-02-03-061.1
608 and the Natural Sciences and Engineering Research Council of Canada (NSERC) through
609 Discovery Grants Program Award RGPIN-2020-05799.

References

- 610
- 611 Arimitsu, M., Piatt, J., & Mueter, F. (2016). Influence of glacier runoff on ecosys-
 612 tem structure in Gulf of Alaska fjords. *Mar. Ecol. Prog. Ser.*, *560*, 19–40. Re-
 613 trieved from <http://www.int-res.com/abstracts/meps/v560/p19-40/> doi:
 614 10.3354/meps11888
- 615 Arrigo, K. R. (2005). Marine microorganisms and global nutrient cycles. *Nature*,
 616 *437*(7057), 349–355. Retrieved from [http://www.nature.com/articles/](http://www.nature.com/articles/nature04159)
 617 [nature04159](http://www.nature.com/articles/nature04159) doi: 10.1038/nature04159
- 618 Bond, N. A., Cronin, M. F., Freeland, H., & Mantua, N. (2015). Causes and impacts
 619 of the 2014 warm anomaly in the NE Pacific. *Geophys. Res. Lett.*, *42*(9), 3414–
 620 3420. Retrieved from <http://doi.wiley.com/10.1002/2015GL063306> doi: 10
 621 .1002/2015GL063306
- 622 Brzezinski, M. A. (1985). The Si:C:N ratio of marine diatoms: interspecific vari-
 623 ability and the effect of some environmental variables. *Journal of Phycol-*
 624 *ogy*, *21*(3), 347–357. Retrieved from [http://doi.wiley.com/10.1111/](http://doi.wiley.com/10.1111/j.0022-3646.1985.00347.x)
 625 [j.0022-3646.1985.00347.x](http://doi.wiley.com/10.1111/j.0022-3646.1985.00347.x) doi: 10.1111/j.0022-3646.1985.00347.x
- 626 *Canadian Tide and Current Tables / Tables des marées et courants du Canada*.
 627 (2019). The Canadian Hydrographic Service, Fisheries and Oceans Canada.
 628 Retrieved from www.charts.gc.ca
- 629 Chandler, P., Foreman, M. G., Ouellet, M., Mimeault, C., & Wade, J. (2017).
 630 *Oceanographic and environmental conditions in the Discovery Islands, British*
 631 *Columbia* (DFO Can. Sci. Advis. Sec. Res. Doc. 2017/071, viii + 51).
- 632 Costalago, D., Forster, I., Nemcek, N., Neville, C., Perry, R. I., Young, K., & Hunt,
 633 B. P. V. (2020). Seasonal and spatial dynamics of the planktonic trophic
 634 biomarkers in the Strait of Georgia (northeast Pacific) and implications
 635 for fish. *Sci Rep*, *10*(1), 8517. Retrieved from [http://www.nature.com/](http://www.nature.com/articles/s41598-020-65557-1)
 636 [articles/s41598-020-65557-1](http://www.nature.com/articles/s41598-020-65557-1) doi: 10.1038/s41598-020-65557-1
- 637 Crawford, W. R., & Peña, M. A. (2013). Declining Oxygen on the British Columbia
 638 Continental Shelf. *Atmosphere-Ocean*, *51*(1), 88–103. Retrieved from [https://](https://www.tandfonline.com/doi/full/10.1080/07055900.2012.753028)
 639 www.tandfonline.com/doi/full/10.1080/07055900.2012.753028 doi: 10
 640 .1080/07055900.2012.753028
- 641 Del Bel Belluz, J., Peña, M., Jackson, J., & Nemcek, M. (2020). Phytoplankton
 642 composition and environmental drivers in the northern Strait of Georgia (Sal-

- 643 ish Sea), British Columbia, Canada. *Estuaries Coast.*
- 644 Di Lorenzo, E., & Mantua, N. (2016). Multi-year persistence of the 2014/15
645 North Pacific marine heatwave. *Nature Clim Change*, *6*(11), 1042–1047.
646 Retrieved from <http://www.nature.com/articles/nclimate3082> doi:
647 10.1038/nclimate3082
- 648 Ebbesmeyer, C. C., & Barnes, C. A. (1980). Control of a fjord basin's dynamics
649 by tidal mixing in embracing sill zones. *Estuarine and Coastal Marine Sci-*
650 *ence*, *11*(3), 311–330. Retrieved from [https://linkinghub.elsevier.com/](https://linkinghub.elsevier.com/retrieve/pii/S0302352480800867)
651 [retrieve/pii/S0302352480800867](https://linkinghub.elsevier.com/retrieve/pii/S0302352480800867) doi: 10.1016/S0302-3524(80)80086-7
- 652 El-Sabaawi, R., Dower, J. F., Kainz, M., & Mazumder, A. (2009). Character-
653 izing dietary variability and trophic positions of coastal calanoid copepods:
654 insight from stable isotopes and fatty acids. *Mar Biol*, *156*(3), 225–237. Re-
655 trieved from <http://link.springer.com/10.1007/s00227-008-1073-1> doi:
656 10.1007/s00227-008-1073-1
- 657 Evans, W., Pocock, K., Hare, A., Weekes, C., Hales, B., Jackson, J., ... Feely, R. A.
658 (2019). Marine CO₂ Patterns in the Northern Salish Sea. *Front. Mar. Sci.*,
659 *5*, 536. Retrieved from <https://www.frontiersin.org/article/10.3389/fmars.2018.00536/full> doi: 10.3389/fmars.2018.00536
- 660
- 661 Feely, R. A., Alin, S. R., Carter, B., Bednaršek, N., Hales, B., Chan, F., ... Ju-
662 ranek, L. (2016). Chemical and biological impacts of ocean acidification along
663 the west coast of North America. *Estuarine, Coastal and Shelf Science*, *183*,
664 260–270. Retrieved from [https://linkinghub.elsevier.com/retrieve/pii/](https://linkinghub.elsevier.com/retrieve/pii/S0272771416302980)
665 [S0272771416302980](https://linkinghub.elsevier.com/retrieve/pii/S0272771416302980) doi: 10.1016/j.ecss.2016.08.043
- 666 Foreman, M., Stucchi, D., Zhang, Y., & Baptiste, A. (2006). Estuarine and Tidal
667 Currents in the Broughton Archipelago. *Atmosphere-Ocean*, *44*(1), 47–63. Re-
668 trieved from <https://www.tandfonline.com/doi/full/10.3137/ao.440104>
669 doi: 10.3137/ao.440104
- 670 Foreman, M., Stucchi, D. J., Garver, K. A., Tuele, D., Isaac, J., Grime, T., ...
671 Morrison, J. (2012). A Circulation Model for the Discovery Islands,
672 British Columbia. *Atmosphere-Ocean*, *50*(3), 301–316. Retrieved from
673 <http://www.tandfonline.com/doi/abs/10.1080/07055900.2012.686900>
674 doi: 10.1080/07055900.2012.686900

- 675 Foreman, M., Sutherland, G., & Cummins, P. (2004). M2 tidal dissipation around
676 Vancouver Island: an inverse approach. *Continental Shelf Research*, *24*(18),
677 2167–2185. Retrieved from [https://linkinghub.elsevier.com/retrieve/
678 pii/S0278434304001700](https://linkinghub.elsevier.com/retrieve/pii/S0278434304001700) doi: 10.1016/j.csr.2004.07.008
- 679 Gay, S. M., & Vaughan, S. L. (2001). Seasonal hydrography and tidal currents
680 of bays and fjords in Prince William Sound, Alaska: Physical oceanogra-
681 phy of nursery habitats of juvenile Pacific herring. *Fisheries Oceanog-
682 raphy*, *10*, 159–193. Retrieved from [http://doi.wiley.com/10.1046/
683 j.1054-6006.2001.00041.x](http://doi.wiley.com/10.1046/j.1054-6006.2001.00041.x) doi: 10.1046/j.1054-6006.2001.00041.x
- 684 Geider, R., & La Roche, J. (2002). Redfield revisited: variability of C:N:P in marine
685 microalgae and its biochemical basis. *European Journal of Phycology*, *37*(1),
686 1–17. Retrieved from [http://www.tandfonline.com/doi/abs/10.1017/
687 S0967026201003456](http://www.tandfonline.com/doi/abs/10.1017/S0967026201003456) doi: 10.1017/S0967026201003456
- 688 Godefroid, M., Boldt, J. L., Thorson, J. T., Forrest, R., Gauthier, S., Flostrand,
689 L., ... Galbraith, M. (2019). Spatio-temporal models provide new in-
690 sights on the biotic and abiotic drivers shaping Pacific Herring (*Clupea pal-
691 lasi*) distribution. *Progress in Oceanography*, *178*, 102198. Retrieved from
692 <https://linkinghub.elsevier.com/retrieve/pii/S0079661119300850>
693 doi: 10.1016/j.pocean.2019.102198
- 694 Godin, G., Candela, J., & de la Paz-Vela, R. (1981). On the feasibility of
695 detecting net transports in and out of Georgia strait with an array of
696 current meters. *Atmosphere-Ocean*, *19*(2), 148–157. Retrieved from
697 <http://www.tandfonline.com/doi/abs/10.1080/07055900.1981.9649106>
698 doi: 10.1080/07055900.1981.9649106
- 699 Griffin, D. A., & LeBlond, P. H. (1990). Estuary/ocean exchange controlled by
700 spring-neap tidal mixing. *Estuarine, Coastal and Shelf Science*, *30*(3), 275–
701 297. Retrieved from [https://linkinghub.elsevier.com/retrieve/pii/
702 027277149090052S](https://linkinghub.elsevier.com/retrieve/pii/027277149090052S) doi: 10.1016/0272-7714(90)90052-S
- 703 Harrison, P. J., Fulton, J. D., Taylor, F. J. R., & Parsons, T. R. (1983). Re-
704 view of the Biological Oceanography of the Strait of Georgia: Pelagic
705 Environment. *Can. J. Fish. Aquat. Sci.*, *40*(7), 1064–1094. Retrieved
706 from <http://www.nrcresearchpress.com/doi/10.1139/f83-129> doi:
707 10.1139/f83-129

- 708 Hibiya, T., & LeBlond, P. H. (1993). The Control of Fjord Circulation by
 709 Fortnightly Modulation of Tidal Mixing Processes. *Journal of Physi-*
 710 *cal Oceanography*, 23(9), 2042–2052. Retrieved from [https://doi.org/](https://doi.org/10.1175/1520-0485(1993)023<2042:TCOFCB>2.0.CO;2)
 711 [10.1175/1520-0485\(1993\)023<2042:TCOFCB>2.0.CO;2](https://doi.org/10.1175/1520-0485(1993)023<2042:TCOFCB>2.0.CO;2) doi: 10.1175/
 712 [1520-0485\(1993\)023\(2042:TCOFCB\)2.0.CO;2](https://doi.org/10.1175/1520-0485(1993)023(2042:TCOFCB)2.0.CO;2)
- 713 Howarth, R. W., & Marino, R. (2006). Nitrogen as the limiting nutrient for
 714 eutrophication in coastal marine ecosystems: Evolving views over three
 715 decades. *Limnol. Oceanogr.*, 51(1 part 2), 364–376. Retrieved from [https://](https://onlinelibrary.wiley.com/doi/abs/10.4319/lo.2006.51.1_part_2.0364)
 716 onlinelibrary.wiley.com/doi/abs/10.4319/lo.2006.51.1_part_2.0364
 717 doi: 10.4319/lo.2006.51.1_part_2.0364
- 718 *Institute of Ocean Sciences Data Archive.* (2020). Ocean Sciences Division, Depart-
 719 ment of Fisheries and Oceans Canada. Retrieved 2018-07-30, from [http://www](http://www.pac.dfo-mpo.gc.ca/science/oceans/data-donnees/index-eng.html)
 720 [.pac.dfo-mpo.gc.ca/science/oceans/data-donnees/index-eng.html](http://www.pac.dfo-mpo.gc.ca/science/oceans/data-donnees/index-eng.html)
- 721 Iriarte, J. L., Pantoja, S., & Daneri, G. (2014). Oceanographic Processes in
 722 Chilean Fjords of Patagonia: From small to large-scale studies. *Progress in*
 723 *Oceanography*, 129, 1–7. Retrieved from [https://linkinghub.elsevier.com/](https://linkinghub.elsevier.com/retrieve/pii/S0079661114001670)
 724 [retrieve/pii/S0079661114001670](https://linkinghub.elsevier.com/retrieve/pii/S0079661114001670) doi: 10.1016/j.pocean.2014.10.004
- 725 Jackson, J. M., Johnson, G. C., Dosser, H. V., & Ross, T. (2018). Warming From
 726 Recent Marine Heatwave Lingers in Deep British Columbia Fjord. *Geophys.*
 727 *Res. Lett.*, 45(18), 9757–9764. Retrieved from [http://doi.wiley.com/](http://doi.wiley.com/10.1029/2018GL078971)
 728 [10.1029/2018GL078971](http://doi.wiley.com/10.1029/2018GL078971) doi: 10.1029/2018GL078971
- 729 James, S. E., Pakhomov, E. A., Mahara, N., & Hunt, B. P. V. (2020). Running
 730 the trophic gauntlet: Empirical support for reduced foraging success in juve-
 731 nile salmon in tidally mixed coastal waters. *Fish Oceanogr.*, 29(3), 290–295.
 732 Retrieved from [https://onlinelibrary.wiley.com/doi/abs/10.1111/](https://onlinelibrary.wiley.com/doi/abs/10.1111/fog.12471)
 733 [fog.12471](https://onlinelibrary.wiley.com/doi/abs/10.1111/fog.12471) doi: 10.1111/fog.12471
- 734 Johannessen, S. C., Masson, D., & Macdonald, R. W. (2014). Oxygen in the deep
 735 Strait of Georgia, 1951-2009: The roles of mixing, deep-water renewal, and
 736 remineralization of organic carbon. *Limnol. Oceanogr.*, 59(1), 211–222. Re-
 737 trieved from <http://doi.wiley.com/10.4319/lo.2014.59.1.0211> doi:
 738 [10.4319/lo.2014.59.1.0211](https://doi.org/10.4319/lo.2014.59.1.0211)
- 739 Khangaonkar, T., Long, W., & Xu, W. (2017). Assessment of circulation and
 740 inter-basin transport in the Salish Sea including Johnstone Strait and Dis-

- 741 covery Islands pathways. *Ocean Modelling*, 109, 11–32. Retrieved from
 742 <https://linkinghub.elsevier.com/retrieve/pii/S1463500316301408>
 743 doi: 10.1016/j.ocemod.2016.11.004
- 744 Klausmeier, C. A., Litchman, E., Daufresne, T., & Levin, S. A. (2008). Phytoplank-
 745 ton stoichiometry. *Ecol Res*, 23(3), 479–485. Retrieved from [http://doi](http://doi.wiley.com/10.1007/s11284-008-0470-8)
 746 [.wiley.com/10.1007/s11284-008-0470-8](http://doi.wiley.com/10.1007/s11284-008-0470-8) doi: 10.1007/s11284-008-0470-8
- 747 Kolmogorov–Smirnov Test. (2008). In *The Concise Encyclopedia of Statis-*
 748 *tics* (pp. 283–287). New York, NY: Springer New York. Retrieved from
 749 http://link.springer.com/10.1007/978-0-387-32833-1_214 doi:
 750 10.1007/978-0-387-32833-1_214
- 751 LeBlond, P. H. (1983). The Strait of Georgia: functional anatomy of a coastal
 752 sea. *Can. J. Fish. Aquat. Sci.*, 40(7), 1033–1063. Retrieved from [http://](http://www.nrcresearchpress.com/doi/10.1139/f83-128)
 753 www.nrcresearchpress.com/doi/10.1139/f83-128 doi: 10.1139/f83-128
- 754 LeBlond, P. H., Ma, H., Doherty, F., & Pond, S. (1991). Deep and intermedi-
 755 ate water replacement in the Strait of Georgia. *Atmosphere-Ocean*, 29(2),
 756 288–312. Retrieved from [http://www.tandfonline.com/doi/abs/10.1080/](http://www.tandfonline.com/doi/abs/10.1080/07055900.1991.9649406)
 757 [07055900.1991.9649406](http://www.tandfonline.com/doi/abs/10.1080/07055900.1991.9649406) doi: 10.1080/07055900.1991.9649406
- 758 Litzow, M., Bailey, K., Prahl, F., & Heintz, R. (2006). Climate regime shifts and re-
 759 organization of fish communities: the essential fatty acid limitation hypothesis.
 760 *Mar. Ecol. Prog. Ser.*, 315, 1–11. Retrieved from [http://www.int-res.com/](http://www.int-res.com/abstracts/meps/v315/p1-11/)
 761 [abstracts/meps/v315/p1-11/](http://www.int-res.com/abstracts/meps/v315/p1-11/) doi: 10.3354/meps315001
- 762 Loder, J. W., Drinkwater, K. F., Oakey, N. S., & Horne, E. P. W. (1994).
 763 Circulation, hydrographic structure and mixing at tidal fronts: the view
 764 from Georges Bank. In H. Charnock, K. R. Dyer, J. M. Huthnance,
 765 P. S. Liss, J. H. Simpson, & P. B. Tett (Eds.), *Understanding the North*
 766 *Sea System* (pp. 69–82). Dordrecht: Springer Netherlands. Retrieved
 767 from http://link.springer.com/10.1007/978-94-011-1236-9_6 doi:
 768 10.1007/978-94-011-1236-9_6
- 769 MacCready, P. (1999). Estuarine Adjustment to Changes in River Flow and Tidal
 770 Mixing. *Journal of Physical Oceanography*, 29(4), 708–726. Retrieved from
 771 [https://doi.org/10.1175/1520-0485\(1999\)029<0708:EATCIR>2.0.CO;2](https://doi.org/10.1175/1520-0485(1999)029<0708:EATCIR>2.0.CO;2)
 772 doi: 10.1175/1520-0485(1999)029(0708:EATCIR)2.0.CO;2

- 773 MacCready, P., & Geyer, W. R. (2010). Advances in Estuarine Physics. *Annu.*
774 *Rev. Mar. Sci.*, 2(1), 35–58. Retrieved from [http://www.annualreviews.org/](http://www.annualreviews.org/doi/10.1146/annurev-marine-120308-081015)
775 [doi/10.1146/annurev-marine-](http://www.annualreviews.org/doi/10.1146/annurev-marine-120308-081015)
776 [-120308-081015](http://www.annualreviews.org/doi/10.1146/annurev-marine-120308-081015) doi: 10.1146/annurev-marine-120308-081015
- 777 MacCready, P., Geyer, W. R., & Burchard, H. (2018). Estuarine Exchange
778 Flow Is Related to Mixing through the Salinity Variance Budget. *Jour-*
779 *nal of Physical Oceanography*, 48(6), 1375–1384. Retrieved from [https://](https://journals.ametsoc.org/jpo/article/48/6/1375/42551/Estuarine-Exchange-Flow-Is-Related-to-Mixing)
780 [journals.ametsoc.org/jpo/article/48/6/1375/42551/Estuarine](https://journals.ametsoc.org/jpo/article/48/6/1375/42551/Estuarine-Exchange-Flow-Is-Related-to-Mixing)
781 [-Exchange-Flow-Is-Related-to-Mixing](https://journals.ametsoc.org/jpo/article/48/6/1375/42551/Estuarine-Exchange-Flow-Is-Related-to-Mixing) doi: 10.1175/JPO-D-17-0266.1
- 782 Mackas, D. L., & Harrison, P. J. (1997). Nitrogenous Nutrient Sources and Sinks in
783 the Juan de Fuca Strait/Strait of Georgia/Puget Sound Estuarine System: As-
784 sessing the Potential for Eutrophication. *Estuarine, Coastal and Shelf Science*,
785 44(1), 1–21. Retrieved from [https://linkinghub.elsevier.com/retrieve/](https://linkinghub.elsevier.com/retrieve/pii/S0272771496901109)
786 [pii/S0272771496901109](https://linkinghub.elsevier.com/retrieve/pii/S0272771496901109) doi: 10.1006/ecss.1996.0110
- 787 Mahara, N., Pakhomov, E. A., Dosser, H. V., & Hunt, B. P. V. (2020). How
788 zooplankton communities are shaped in a complex and dynamic coastal sys-
789 tem with strong tidal influence. *Estuarine, Coastal and Shelf Science*. doi:
790 10.1016/j.ecss.2020.107103
- 791 Masson, D. (2002). Deep Water Renewal in the Strait of Georgia. *Estuar-*
792 *ine, Coastal and Shelf Science*, 54(1), 115–126. Retrieved from [https://](https://linkinghub.elsevier.com/retrieve/pii/S0272771401908339)
793 linkinghub.elsevier.com/retrieve/pii/S0272771401908339 doi:
794 10.1006/ecss.2001.0833
- 795 Masson, D., & Cummins, P. F. (2004). Observations and modeling of seasonal
796 variability in the Straits of Georgia and Juan de Fuca. *J Mar Res*, 62(4),
797 491–516. Retrieved from [http://www.ingentaselect.com/rpsv/cgi-bin/](http://www.ingentaselect.com/rpsv/cgi-bin/cgi?ini=xref&body=linker&reqdoi=10.1357/0022240041850075)
798 [cgi?ini=xref&body=linker&reqdoi=10.1357/0022240041850075](http://www.ingentaselect.com/rpsv/cgi-bin/cgi?ini=xref&body=linker&reqdoi=10.1357/0022240041850075) doi:
799 10.1357/0022240041850075
- 800 Masson, D., & Peña, A. (2009). Chlorophyll distribution in a temperate estuary:
801 The Strait of Georgia and Juan de Fuca Strait. *Estuarine, Coastal and Shelf*
802 *Science*, 82(1), 19–28. Retrieved from [https://linkinghub.elsevier.com/](https://linkinghub.elsevier.com/retrieve/pii/S027277140900002X)
803 [retrieve/pii/S027277140900002X](https://linkinghub.elsevier.com/retrieve/pii/S027277140900002X) doi: 10.1016/j.ecss.2008.12.022
- 804 McKinnell, S., Curchitser, E., Groot, K., Kaeriyama, M., & Trudel, M. (2014).
805 Oceanic and atmospheric extremes motivate a new hypothesis for variable

- 806 marine survival of Fraser River sockeye salmon. *Fish. Oceanogr.*, *23*(4), 322–
807 341. Retrieved from <http://doi.wiley.com/10.1111/fog.12063> doi:
808 10.1111/fog.12063
- 809 Murray, J. W., Roberts, E., Howard, E., O'Donnell, M., Bantam, C., Carrington, E.,
810 ... Fay, A. (2015). An inland sea high nitrate-low chlorophyll (HNLC) region
811 with naturally high pCO₂. *Limnol. Oceanogr.*, *60*(3), 957–966. Retrieved
812 from <https://onlinelibrary.wiley.com/doi/10.1002/lno.10062> doi:
813 10.1002/lno.10062
- 814 Olson, E. M., Allen, S. E., Do, V., Dunphy, M., & Ianson, D. (2020). Assessment
815 of Nutrient Supply by a Tidal Jet in the Northern Strait of Georgia Based
816 on a Biogeochemical Model. *J. Geophys. Res. Oceans*, *125*(8). Retrieved
817 from <https://onlinelibrary.wiley.com/doi/10.1029/2019JC015766> doi:
818 10.1029/2019JC015766
- 819 Park, K., & Kuo, A. Y. (1996). Effect of variation in vertical mixing on resid-
820 ual circulation in narrow, weakly nonlinear estuaries. In D. G. Aubrey &
821 C. T. Friedrichs (Eds.), *Coastal and Estuarine Studies* (Vol. 53, pp. 301–
822 317). Washington, D. C.: American Geophysical Union. Retrieved from
823 <http://www.agu.org/books/ce/v053/CE053p0301/CE053p0301.shtml> doi:
824 10.1029/CE053p0301
- 825 Pawlowicz, R., Riche, O., & Halverson, M. (2007). The circulation and residence
826 time of the strait of Georgia using a simple mixing-box approach. *Atmosphere-*
827 *Ocean*, *45*(4), 173–193. Retrieved from [http://www.tandfonline.com/doi/](http://www.tandfonline.com/doi/abs/10.3137/ao.450401)
828 [abs/10.3137/ao.450401](http://www.tandfonline.com/doi/abs/10.3137/ao.450401) doi: 10.3137/ao.450401
- 829 Riche, O., Johannessen, S., & Macdonald, R. (2014). Why timing matters in
830 a coastal sea: Trends, variability and tipping points in the Strait of Geor-
831 gia, Canada. *Journal of Marine Systems*, *131*, 36–53. Retrieved from
832 <https://linkinghub.elsevier.com/retrieve/pii/S092479631300225X>
833 doi: 10.1016/j.jmarsys.2013.11.003
- 834 Smethie, W. M. (1987). Nutrient regeneration and denitrification in low oxygen
835 fjords. *Deep Sea Research Part A. Oceanographic Research Papers*, *34*(5-6),
836 983–1006. Retrieved from [https://linkinghub.elsevier.com/retrieve/](https://linkinghub.elsevier.com/retrieve/pii/0198014987900495)
837 [pii/0198014987900495](https://linkinghub.elsevier.com/retrieve/pii/0198014987900495) doi: 10.1016/0198-0149(87)90049-5

- 838 Stanton, B. R., & Pickard, G. L. (1980). Physical Oceanography of the New
839 Zealand Fjords. In H. J. Freeland, D. M. Farmer, & C. D. Levings (Eds.),
840 *Fjord Oceanography* (pp. 329–332). Boston, MA: Springer US. Retrieved
841 from http://link.springer.com/10.1007/978-1-4613-3105-6_26 doi:
842 10.1007/978-1-4613-3105-6_26
- 843 Strom, S., Olson, M., Macri, E., & Mord, C. (2006). Cross-shelf gradients in phy-
844 toplankton community structure, nutrient utilization, and growth rate in
845 the coastal Gulf of Alaska. *Mar. Ecol. Prog. Ser.*, *328*, 75–92. Retrieved
846 from <http://www.int-res.com/abstracts/meps/v328/p75-92/> doi:
847 10.3354/meps328075
- 848 Sutton, J. N., Johannessen, S. C., & Macdonald, R. W. (2013). A nitrogen budget
849 for the Strait of Georgia, British Columbia, with emphasis on particulate ni-
850 trogen and dissolved inorganic nitrogen. *Biogeosciences*, *10*(11), 7179–7194.
851 Retrieved from <https://bg.copernicus.org/articles/10/7179/2013/> doi:
852 10.5194/bg-10-7179-2013
- 853 Svendsen, H. (1995). Physical oceanography of coupled fjord-coast systems in
854 northern Norway with special focus on frontal dynamics and tides. In *Ecology*
855 *of fjords and coastal waters: proceedings of the Mare Nor Symposium on the*
856 *Ecology of Fjords and Coastal Waters, Tromsø, Norway, 5-9 December, 1994*
857 (pp. 149–164). Amsterdam ; New York: Elsevier. (Meeting Name: Mare Nor
858 Symposium on the Ecology of Fjords and Coastal Waters)
- 859 Thomson, R. E. (1976). Tidal Currents and Estuarine-Type Circulation in John-
860 stone Strait, British Columbia. *J. Fish. Res. Bd. Can.*, *33*(10), 2242–2264. Re-
861 trieved from <http://www.nrcresearchpress.com/doi/10.1139/f76-272> doi:
862 10.1139/f76-272
- 863 Thomson, R. E. (1981). *Oceanography of the British Columbia coast* (Vol. 56). Can.
864 Spec. Publ. Fish. Aquat. Sci.
- 865 Thomson, R. E., & Huggett, W. S. (1980). M2 Baroclinic Tides in Johnstone
866 Strait, British Columbia. *Journal of Physical Oceanography*, *10*(10), 1509–
867 1539. Retrieved from [https://doi.org/10.1175/1520-0485\(1980\)010<1509:MBTIJS>2.0.CO;2](https://doi.org/10.1175/1520-0485(1980)010<1509:MBTIJS>2.0.CO;2) doi:
868 10.1175/1520-0485(1980)010<1509:MBTIJS>2.0.CO;2
- 869 Thomson, R. E., & Krassovski, M. V. (2010). Poleward reach of the Califor-
870 nia Undercurrent extension. *J. Geophys. Res.*, *115*(C9), C09027. Re-

- 871 trieved from <http://doi.wiley.com/10.1029/2010JC006280> doi:
872 10.1029/2010JC006280
- 873 van Heijst, G. (1986). On the Dynamics of a Tidal Mixing Front. In *Elsevier*
874 *Oceanography Series* (Vol. 42, pp. 165–194). Elsevier. Retrieved from
875 <https://linkinghub.elsevier.com/retrieve/pii/S0422989408710456>
876 doi: 10.1016/S0422-9894(08)71045-6
- 877 Waldichuk, M. (1957). Physical Oceanography of the Strait of Georgia, British
878 Columbia. *J. Fish. Res. Bd. Can.*, 14(3), 321–486. Retrieved from [http://www](http://www.nrcresearchpress.com/doi/10.1139/f57-013)
879 [.nrcresearchpress.com/doi/10.1139/f57-013](http://www.nrcresearchpress.com/doi/10.1139/f57-013) doi: 10.1139/f57-013
- 880 Ware, D. M., & McFarlane, G. A. (1989). *Fisheries production domains in the*
881 *Northeast Pacific Ocean*. (Can. Spec. Publ. Fish. Aquat. Sci. No. 108).
- 882 Whitney, F., Crawford, W., & Harrison, P. (2005). Physical processes that
883 enhance nutrient transport and primary productivity in the coastal and
884 open ocean of the subarctic NE Pacific. *Deep Sea Research Part II: Topi-*
885 *cal Studies in Oceanography*, 52(5-6), 681–706. Retrieved from [https://](https://linkinghub.elsevier.com/retrieve/pii/S0967064505000044)
886 linkinghub.elsevier.com/retrieve/pii/S0967064505000044 doi:
887 10.1016/j.dsr2.2004.12.023